Targeting Macrophage Histone H3 Modification as a Leishmania Strategy to Dampen the NF-κB/NLRP3-Mediated Inflammatory Response

Hervé Lecoeur, Eric Prina, Thibault Rosazza, Kossiwa Kokou, Paya N'Diaye, Nathalie Aulner, Hugo Varet, Giovanni Bussotti, Yue Xing, Geneviève Milon, et al.

Article

Cell Reports

Targeting Macrophage Histone H3 Modification as a *Leishmania* Strategy to Dampen the NF-κB/NLRP3-Mediated Inflammatory Response

Graphical Abstract

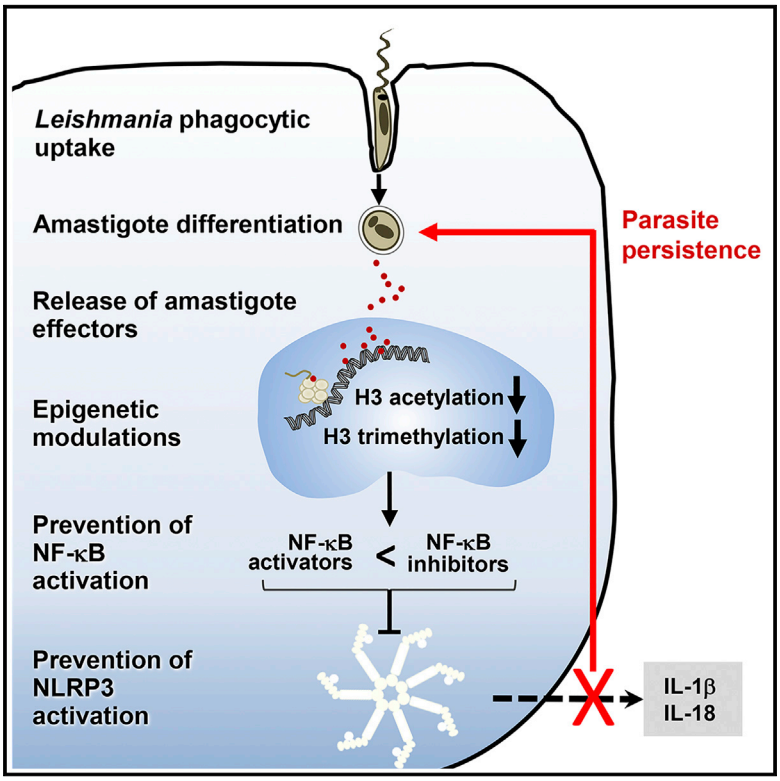

Highlights

- *Leishmania* modulates H3 modification of macrophages *in vitro* and *in vivo*
- *Leishmania* prevents NF-κB and NLRP3 activation in infected macrophages
- *Leishmania* induces long-term transcriptomic modulations of NF-κB and NLRP3 pathways

Authors

Hervé Lecoeur, Eric Prina, Thibault Rosazza, ..., Robert Weil, Guangxun Meng, Gerald F. Späth

Correspondence

gerald.spaeth@pasteur.fr

In Brief

Lecoeur et al. demonstrate that the parasite *Leishmania amazonensis* modifies expression of NF-kB-related genes and prevents NLRP3 inflammasome activation of host macrophages *in vitro* and *in vivo* by changing histone H3 modifications at the promotor of pro-inflammatory genes. This mechanism of immune subversion opens avenues for host-directed, anti-leishmanial therapies.

Lecoeur et al., 2020, Cell Reports *30*, 1870–1882
February 11, 2020
https://doi.org/10.1016/j.celrep.2020.01.030

CellPress

OPEN ACCESS
CellPress

Cell Reports
Article

Targeting Macrophage Histone H3 Modification as a *Leishmania* Strategy to Dampen the NF-κB/NLRP3-Mediated Inflammatory Response

Hervé Lecoeur,[1,2,3,8] Eric Prina,[1,3,8] Thibault Rosazza,[1,3] Kossiwa Kokou,[1,2,3] Paya N'Diaye,[1] Nathalie Aulner,[4] Hugo Varet,[5] Giovanni Bussotti,[5] Yue Xing,[2,3] Geneviève Milon,[6] Robert Weil,[7] Guangxun Meng,[2,3] and Gerald F. Späth[1,3,9,*]

[1]INSERM U1201, Unité de Parasitologie Moléculaire et Signalisation, Département des Parasites et Insectes Vecteurs, Institut Pasteur, 25 Rue du Dr Roux, 75015 Paris, France
[2]Institut Pasteur of Shanghai, The Center for Microbes, Development and Health, Key Laboratory of Molecular Virology & Immunology, Chinese Academy of Sciences, Shanghai 200031, China
[3]Institut Pasteur International Mixed Unit "Inflammation and *Leishmania* infection," Paris, France
[4]Unité de Technologie et de Services Photonic BioImaging, Centre de Recherche et de Ressources Technologiques, Direction de la Technologie et des Programmes Scientifiques, Institut Pasteur, 28 Rue du Dr Roux, 75015 Paris, France
[5]Hub de Bioinformatique et Biostatistique, Département Biologie Computationnelle, Institut Pasteur, USR 3756 CNRS, Paris, France
[6]Institut Pasteur, 25 Rue du Dr Roux, 75015 Paris, France
[7]Sorbonne Universités, Institut National de la Santé et de la Recherche Médicale (INSERM, UMR1135), Centre National de la Recherche Scientifique (CNRS, ERL8255), Centre d'Immunologie et des Maladies Infectieuses CIMI, Paris, France
[8]These authors contributed equally
[9]Lead Contact
*Correspondence: gerald.spaeth@pasteur.fr
https://doi.org/10.1016/j.celrep.2020.01.030

SUMMARY

Aberrant macrophage activation during intracellular infection generates immunopathologies that can cause severe human morbidity. A better understanding of immune subversion strategies and macrophage phenotypic and functional responses is necessary to design host-directed intervention strategies. Here, we uncover a fine-tuned transcriptional response that is induced in primary and lesional macrophages infected by the parasite *Leishmania amazonensis* and dampens NF-κB and NLRP3 inflammasome activation. Subversion is amastigote-specific and characterized by a decreased expression of activating and increased expression of de-activating components of these pro-inflammatory pathways, thus revealing a regulatory dichotomy that abrogates the anti-microbial response. Changes in transcript abundance correlate with histone H3K9/14 hypoacetylation and H3K4 hypo-trimethylation in infected primary and lesional macrophages at promoters of NF-κB-related, pro-inflammatory genes. Our results reveal a *Leishmania* immune subversion strategy targeting host cell epigenetic regulation to establish conditions beneficial for parasite survival and open avenues for host-directed, anti-microbial drug discovery.

INTRODUCTION

Macrophages are phagocytic cells of the reticulo-endothelial system that carry out a plethora of functions, including maintenance of tissue-specific homeostasis and repair, destruction of microbial pathogens by innate, cytolytic activities, and activation of appropriate immune responses against cancer or infectious agents (Ginhoux and Jung, 2014; Gordon and Taylor, 2005). This functional diversity is matched by an equally diverse phenotypic landscape, with macrophages acquiring distinct and unique morphological and functional properties in response to tissue-specific determinants or interactions with tumor cells and microbes (Biswas and Mantovani, 2010; Gordon and Martinez, 2010). Although this plasticity adapts the macrophage response to very diverse physiological and microbial insults, aberrant polarization has been linked to various pathologies, in particular during intracellular infection (Murray et al., 2014). Many viral, bacterial, and eukaryotic pathogens exploit macrophages as host cells and have co-evolved strategies to modulate the macrophage phenotype promoting their own survival (Benoit et al., 2008; Gazzinelli et al., 2014; Herbein and Varin, 2010; Herbert et al., 2004; Noël et al., 2004; Pathak et al., 2007; Pearce and MacDonald, 2002; Raes et al., 2007). Intracellular pathogens thus are a major threat to human health, but also represent interesting tools to probe macrophage plasticity and understand its role in the pathophysiology of infection. This is well exemplified by the intracellular parasite *Leishmania*, which has been used as a model pathogen to gain insight into innate and acquired immune response pathways that govern resistance or susceptibility to microbial infection (Bellamy, 1999; Canonne-Hergaux et al., 1999; Sacks and Noben-Trauth, 2002; Scott and Farrell, 1981, 1982).

Protist pathogens of the genus *Leishmania* cause severe immunopathologies in humans and animals termed leishmaniases (Alvar et al., 2012). Following transmission of the insect-stage promastigote form of the parasite to vertebrate hosts by blood-feeding infected sand flies, the parasite develops into

the amastigote form inside the fully acidified phagolysosomes of host macrophages (Antoine et al., 1998; Zilberstein and Shapira, 1994). Intracellular amastigotes manipulate host cell signaling, immune functions, and metabolism to establish permissive conditions for long-term chronic infection (Arango Duque and Descoteaux, 2015; Giraud et al., 2012; Lecoeur et al., 2010; Lecoeur et al., 2013; McConville et al., 2015; Olivier et al., 2005; Osorio y Fortéa et al., 2007, 2009). In recent years, the impact of intracellular *Leishmania* infection on the NF-κB-mediated and inflammasome-dependent pro-inflammatory response has attracted important attention. NF-κB denotes a eukaryotic protein family of related transcription factors that form various homo- and heterodimeric complexes involved in regulating promoter activities during inflammation, including the pro-inflammatory cytokines interleukin-1β (IL-1β), interleukin-18 (IL-18), and the NLRP3 inflammasome (He et al., 2016). The inflammasome represents a series of related multi-protein complexes defined by specific Nod-like receptor proteins that lead to caspase-1-dependent maturation of pro-IL-1β and pro-IL-18 (Franchi et al., 2012), thus placing this pathway downstream of NF-κB (Jo et al., 2016). Despite the plethora of studies investigating *Leishmania* anti- and pro-inflammatory activities, little is known of the mechanisms that modulate NF-κB-regulated and inflammasome-dependent gene expression in *Leishmania*-infected macrophages, and how the plasticity of the macrophage response is exploited by this pathogen to favor its intracellular survival.

Here, by using primary murine macrophages infected with bona fide *L. amazonensis* (*L. am*) amastigotes *in vitro*, and lesion-derived macrophages infected *in vivo*, we provide first insight into a parasite immune subversion mechanism targeting histone H3 post-translational modifications. Unlike *Leishmania* insect-stage promastigotes (Dey et al., 2018; Gurung et al., 2015; Lima-Junior et al., 2013), we show that amastigotes cause transcriptional inhibition of the host cell pro-inflammatory responses via a dichotomic regulation of activators and inhibitors of the NF-κB-NLRP3 axis.

RESULTS

L. am Amastigotes Prevent Inflammasome Priming and Activation

The macrophage inflammasome response to *L. am* infection has been previously studied using insect-stage promastigotes derived from *in vitro* culture (Lima-Junior et al., 2013). Here we assess the impact of disease-relevant, bona fide *L. am* amastigotes on inflammasome priming and activation in primary, bone marrow-derived murine macrophages (BMDMs). Unlike LPS/ATP-treated controls, BMDM infection with lesion-derived *L. am* amastigotes did not lead to inflammasome activation, as judged by the absence of secretion of mature IL-1β and active caspase-1 p20 (Figure 1A) and ASC oligomerization (Figure 1B). On the contrary, infection caused a significant reduction of all major inflammasome receptor proteins, including NLRP3, NLRC4, AIM2, and RIG-1 (Figure 1C). This was consistent with a similar reduction in transcript abundance in response to live but not heat-killed parasites or inert latex beads (Figure 1D). Downregulation was specific to amastigotes, as judged by normal abundance of *il1β*, *il18*, and *nlrp3* transcripts 24 h after infection with purified metacyclic promastigotes (Figures S1A and S1B) and the reduction of these transcripts after intracellular amastigote differentiation 3 days post-infection (PI) (Figures S1A and S1B), which reproduced the inhibitory effects observed with lesion-derived amastigotes. Decreased levels of *il1β* and *il18* transcripts correlated with increased amastigote burden during long-term cultures (30 days of infection; Figures 1E and 1F; Figure S1C). Significantly, long-term infection had no effect on macrophage phagocytic activity, surface marker expression (Figure S1D), or transcript expression of various inflammasome-independent cytokines, including *il1α* and *tnf* (Figures S1E and S1F), while a persistent down-modulation of transcripts for additional inflammasome components was induced (Figure S1G).

We next assessed the capacity of *L. am* amastigotes to inhibit priming and activation of the NLRP3 inflammasome in response to sequential LPS and ATP stimulation. Our results demonstrate that *L. am* infection interfered with inflammasome activation on multiple levels, as judged by (1) the reduction of active caspase-1 p20 in the supernatant and accumulation of inactive pro-caspase-1 in the cytoplasm (Figure 1G), (2) the decrease in protein abundance of NLRP3, RIG-1, and AIM2 inflammasomes (Figure 1G), and (3) the reduction of IL-1β and IL-18 secretion (Figures 1H and 1I), which was independent of the duration and concentration of ATP stimulation (data not shown). In agreement with our observations in unstimulated macrophages, the subversion of inflammasome priming and activation in LPS/ATP-stimulated macrophages was amastigote specific, as metacyclic promastigotes did not interfere with the secretion or the transcriptional modulation of IL-1β and IL-18 until they differentiated into amastigotes (day 3 PI) (Figure S2). Interestingly, amastigote infection did not modify IL-1α secretion or transcript stability (Figures S3A and S3C), but it increased the production of pro-inflammatory TNF (Figure S3B). This could result from increased *tnf* mRNA stability (Figure S3D) and other NF-κB-independent mechanisms (Falvo et al., 2010). In conclusion, our data demonstrate that *L. am* amastigotes specifically inhibit the basal and LPS/ATP-induced expression level of inflammasome components and their target cytokines by an active, parasite-driven, and stage-specific mechanism.

Pleiotropic Inhibition of the NF-κB Pathway by *L. am* Amastigotes

We next investigated the impact of *L. am* amastigote infection on the activity of NF-κB p65 (RelA), a master regulator of the inflammatory response that has been shown crucial for the priming step of NLRP3 activation and IL-1β and IL-18 expression (Jo et al., 2016). The analysis of the NF-κB pathway in uninfected and *L. am*-infected BMDMs revealed inhibition of this pathway by the intracellular parasites at multiple levels. First, using a high-content quantitative imaging approach, we observed a highly significant reduction in the nuclear localization of RelA in infected macrophages compared with uninfected controls in the absence or presence of pro-inflammatory stimuli (Figures 2A and 2B). Second, we revealed a 2-fold decrease in total RelA protein expression in infected cells regardless of lipopolysaccharide (LPS) treatment (Figure 2C), which partially explained its reduced nuclear abundance. Third, by treating cells with the proteasome inhibitor MG132, we showed that infection reduced

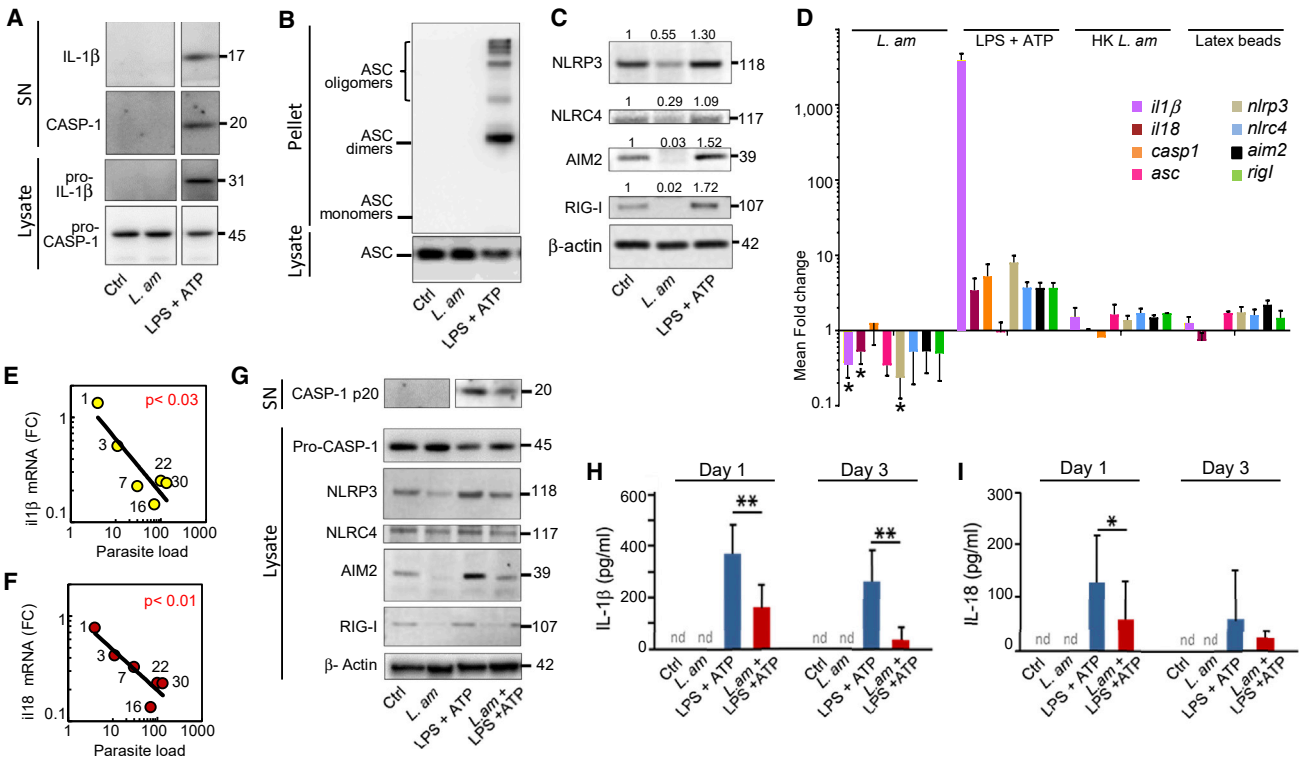

Figure 1. Prevention of Inflammasome Priming and Activation in *L. am*-Infected Macrophages

BMDMs were infected with amastigotes at a MOI of 4:1.

(A) Western blot analysis of mature IL-1β and caspase-1 p20 in culture supernatants (SN) and pro-caspase-1 and pro-IL-1β in macrophage lysates (day 3 PI).

(B) Western blot analysis of ASC in cell lysates and pellets (day 3 PI).

(C) Western blot analysis of NLRP3, NLRC4, AIM2, and RIG-1 inflammasomes in BMDM lysates (day 3 PI). Beta-actin was used as a control protein.

(D) Transcriptional modulation of inflammasome components as assessed by qRT-PCR. BMDMs were loaded with live (*L. am*) or heat-killed (HK *L. am*) amastigotes or latex beads and cultured for 3 days. As positive control, NLRP3 activation was induced after LPS and ATP stimulation. The expression fold changes (FCs) are indicated using uninfected and unstimulated macrophages as a calibrator. Histograms display mean FC values ± SEM for *L. am*-infected and LPS + ATP-treated uninfected BMDMs (n = 4–13 independent experiments) and for HK *L. am* and latex bead-loaded BMDMs (technical duplicates; one representative experiment is shown).

(E and F) Biparametric dot plots displaying transcript modulation (fold changes [FCs]) of IL-1β (E) and IL-18 (F) and parasite load (mean number of amastigotes per macrophage) at different time points PI (indicated by the numeric label of the data points). The F-test p value is indicated for the corresponding linear regression.

(G) Western blot analyses of inflammasome components at day 3 PI in culture supernatants (SN) and lysates from LPS-stimulated and non-stimulated samples.

(H and I) Detection by ELISA of secreted IL-1β (H) and IL-18 (I). Cytokines were quantified in supernatants following sequential LPS/ATP stimulation of macrophages at day 1 and day 3 PI. Blue and red bars represent cytokine levels for uninfected and infected BMDMs, respectively (mean ± SEM, n = 3-6). nd, not detected; *p < 0.06; **p < 0.05.

the phosphorylation levels of the NF-κB inhibitor IκBα in response to LPS, thus stabilizing the protein and further dampening NF-κB activation (Figure 2D). Reduced IκBα phosphorylation was correlated with reduced protein abundance of the IκB protein kinase (IKKβ) in *L. am*-infected BMDMs (Figure 2D). As judged by qRT-PCR, the decreased protein level is the consequence of reduced expression of *rela*, *iκbα*, and *ikkβ* transcripts in the absence (Figure 2E) or presence (Figure 2F) of a short pulse (30 min) of LPS. Strong inhibition was also observed for other NF-κB family members (*relb* [p50], *nf-κb1*, and *nf-κb2*) and the NF-κB activators *ikkα* and *ikkγ*, which persisted during long-term infection (Figure S4). Finally, we also observed a low abundance of transcripts for *iκbα*, *iκbβ*, and *iκbε*, which are part of a negative feedback loop involved in the termination of NF-κB activation (Renner and Schmitz, 2009).

Transcript Profiling Reveals Dichotomic Inhibition of the NF-κB-NLRP3 Axis by *L. am* Amastigotes

Given the pleiotropic effect of *L. am* amastigotes on the NF-κB pathway, we extended our transcript analysis using qRT-PCR to investigate the impact of infection on the expression of 97 components of the NF-κB/NLRP3 axis (Figure 3). We revealed a surprising dichotomic transcriptional pattern. On one hand, infection reduced expression of positive regulators of the NF-κB pathway, including the pro-inflammatory surface receptors *il18r1* ($\log_2$ fold change [FC] = −1.83), *tnfrsf1A* ($\log_2$ FC = −1.04), *tlr4* ($\log_2$ FC = −0.64), the *myd88* adaptor ($\log_2$ FC = −0.57), and kinases such as *irak4* ($\log_2$ FC = −0.77) and *mapk14* ($\log_2$ FC = −0.98). On the other hand, infection upregulated transcripts of anti-inflammatory molecules and known inhibitors of NF-κB activation such as *tollip* ($\log_2$ FC = +0.95) and *otud7b* ($\log_2$ FC = +2.08) (Figure 3A; Figure S5). A

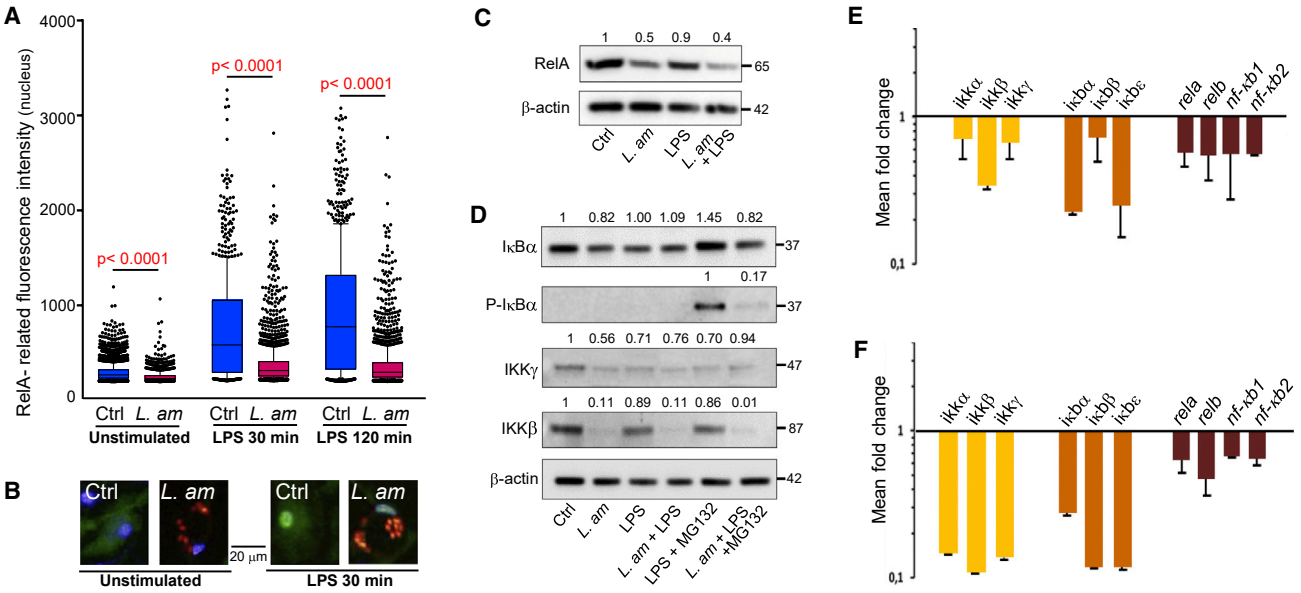

Figure 2. Subversion of the NF-κB Pathway in *L. am*-Infected BMDMs

BMDMs were infected by lesional *L. am* amastigotes. At 3 days PI, uninfected (Ctrl) and infected (*L. am*) BMDMs were stimulated or not with LPS for 30 or 120 min.

(A) Quantitative evaluation of nuclear translocation of RelA (p65) by using high-content imaging. RelA was evidenced using an anti-RelA polyclonal antibody and an Alexa Fluor 488 conjugate (green staining). Cell nuclei were stained with Hoechst 33342, and parasites were visualized by using mCherry fluorescence (red staining). Image acquisition and analysis were performed using the OPERA QEHS and the Columbus image storage and analysis system, respectively. The mean fluorescence intensity of RelA-associated staining in BMDM nuclei after 30 and 120 min of LPS stimulation is shown (blue and red box-and-whisker plots, respectively) (800 < analyzed nuclei < 2,000).

(B) Representative images are shown. Note the moderate green (RelA-related) staining in nuclei from infected versus uninfected BMDMs.

(C and D) Relative quantitation by western blot analysis of selected key actors of the NF-κB pathway in total protein extracts. At 3 days PI, BMDM cultures were stimulated sequentially with LPS (4 h) and ATP (2 h). The following proteins were analyzed: RelA (C), IκBα and its phosphorylated form (P- IκBα), IKKγ, and IKKβ (D). MG132 was added to prevent proteasomal degradation, allowing the revelation of phosphorylated IκBα.

(E and F) Transcript modulations of NF-κB members in *L. am*-infected BMDMs. qRT-PCR was performed in samples without LPS (E) (n = 3 experiments) or after 30 min of LPS stimulation (F) (n = 1 representative experiment). Results are shown as fold change values obtained between infected and uninfected BMDMs (calibrator) for members of the signalosome (*ikkα*, *ikkβ*, and *ikkγ*; yellow bars), kinases (*iκbα*, *iκbβ*, and *iκbε*; orange bars), and NF-κB family members (*rela*, *relb*, *nfκb1*, and *nfκb2*; brown bars).

similar regulatory dichotomy was observed for a series of known NLRP3 activators (*p2rx7*; $\log_2$ FC = −1.63) and inhibitors (*tnfaip3*; $\log_2$ FC = +1.84) (Figure 3B).

A slightly different pattern was observed in infected cells stimulated by LPS/ATP: although the down-modulation of NF-κB positive regulators remained robust, no significant effect on inhibitory components was observed (Figure 3C; Figure S5), which may explain the dampening rather than abrogation of inflammasome activation we observed in LPS/ATP-stimulated, infected BMDMs. Together these data uncover a surprisingly fine-tuned modulation of the host cell transcriptome during *L. am* infection that relies on a pleotropic, yet highly regulated inhibition of inflammatory responses through antagonistic regulation of pro- and anti-inflammatory genes.

Modulation of the Level of Macrophage Histone H3 Acetylation and Methylation during *L. am* Infection

As histone acetylation is crucial for the regulation of NF-κB-mediated inflammation (Ghizzoni et al., 2011), we next investigated if the dichotomic transcriptomic modulation of pro- and anti-inflammatory genes during *L. am* infection was linked to epigenetic regulation. Using EpiTect chromatin immunoprecipitation (ChIP) qPCR arrays, changes in the histone H3 activation marks H3K9/14 acetylation, H3K4, and H3K9 trimethylation were assessed on a focused panel of 88 NF-κB-associated gene promoters (for the correlation between independent experiments, see Figures S6A and S6B). Even though infection alone did not affect the H3 K9/14 acetylation level in unstimulated macrophages (Figure S6C), parasite infection caused a reproducible hypoacetylation at the level of various pro-inflammatory promoters (Figure 4A), which correlated with the decreased abundance of the corresponding transcripts (see Figure 3), including TLR9, MYD88, and the NF-κB member RelA. Likewise, a correlation between increased H3 acetylation and transcript expression levels was observed among upregulated genes, for example, for the NF-κB negative regulator TNFAIP3, which plays a pivotal role in the termination of NF-κB-induced inflammation (Pujari et al., 2013). Thus, the dichotomy observed on transcript levels is largely reproduced on the level of H3 acetylation. Histone H3 hypoacetylation observed at pro-inflammatory promoters further correlated with a significant reduction of another epigenetic activation mark, H3K4 trimethylation (Figures S6D and S6E), while no significant changes were observed for the H3K9 trimethylation mark (Figure S6F).

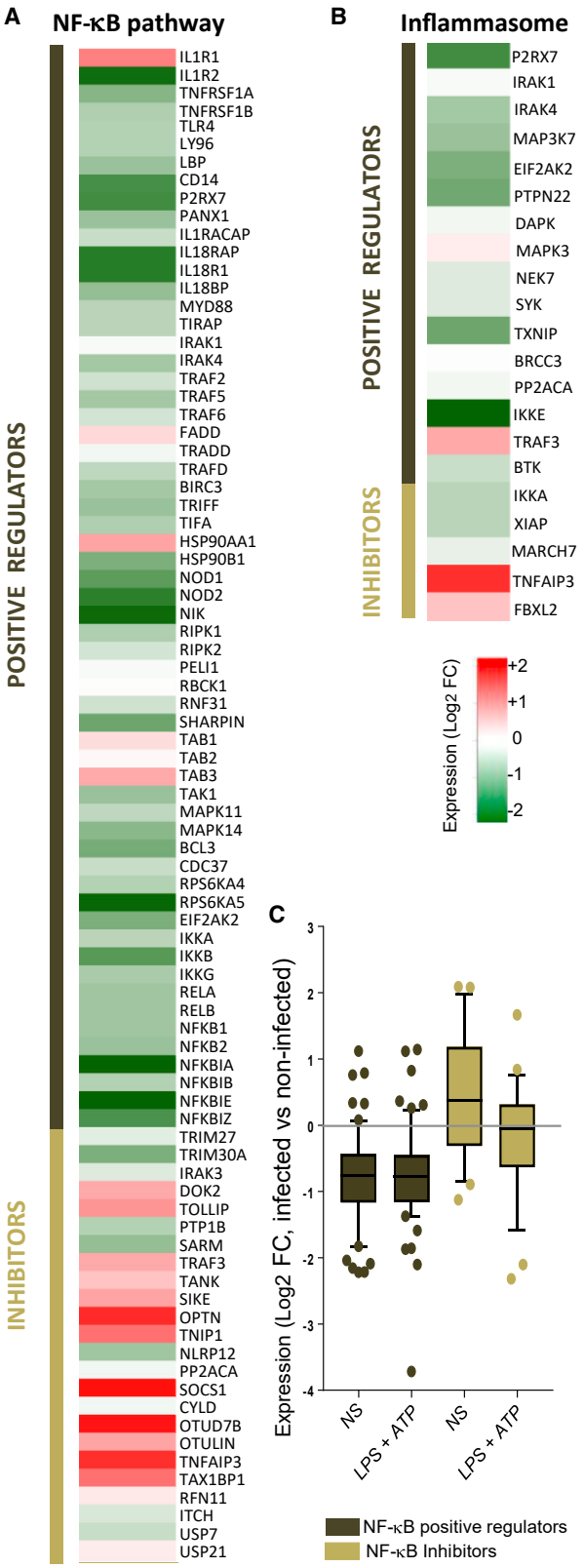

Figure 3. Transcriptional Regulatory Dichotomy of the NF-κB Signaling Pathway in *L. am*-Infected Macrophages

After 3 days PI, total RNA from uninfected and *L. am*-infected BMDMs was isolated and reverse transcribed. cDNA was subjected to qRT-PCR analysis targeting components of the NF-κB and NLRP3 pathways.

(A and B) Log_2 values of fold changes in transcript abundance are represented as heatmaps (infected versus uninfected BMDMs) for activators and inhibitors of the NF-κB (A) and inflammasome (B) pathways (mean, $3 < n < 8$ independent experiments).

(C) Comparison of global transcriptional modulation induced by *L. am* parasites in unstimulated (NS) or LPS/ATP-stimulated BMDMs for activators (dark brown) and inhibitors (light brown) of the NF-κB pathway. Box-and-whisker plots represent the mean and the 10th to 90th percentiles of the log_2 fold change values.

As expected from previous reports (Kapellos and Iqbal, 2016; Saeed et al., 2014), LPS treatment caused a strong global increase in H3K9/14 acetylation in uninfected controls, which was significantly reduced during *L. am* infection (Figure S6C). Similar to the results obtained on transcript levels, such an epigenetic dichotomy was not observed in LPS-activated macrophages for the promoters we analyzed: although the reduced acetylation observed for NF-κB positive regulators remained robust, no significant effect on inhibitory components was seen (Figure 4B), which explains the dampening rather than the abrogation of inflammasome activation. Nevertheless, *L. am* infection efficiently counteracted the increase in H3 acetylation caused by LPS, with H3 hypoacetylation demonstrated, for example, at the promoter level for the NF-κB inhibitor TNFAIP3. Overall, the global prevention of LPS-mediated H3 acetylation far exceeded the effect observed in unstimulated macrophages demonstrating the capacity of intracellular *L. am* to most efficiently interfere with the pro-inflammatory host cell response (Figure 4C).

Lesion-Derived, *L. am*-Infected Macrophages Display an Anti-inflammatory Phenotype

We established a new protocol to assess the phenotype of *L. am*-infected tissue monocytes/macrophages *ex vivo*. Two months after infection with mCherry-transgenic *L. am* parasites, lesional macrophages were isolated from footpads of BALB/c nude mice after gentle perfusion of the infected tissue with a cocktail of dispase II, collagenases II and IV, and DNase I. This novel procedure allowed us to recover heavily infected monocytes/macrophages that showed a substantial increase in cell area compared with the few non-infected cells present in the same sample (Figures 5A and 5B). The response of these *ex vivo* cells was compared with that of non-infected BMDMs that we used as a benchmark for macrophage activation, given that our procedure was unable to purify sufficient amounts of macrophages, unlike previous studies in which uninfected cells from mouse ears were used for single-cell analyses (Lee et al., 2018). Lesional macrophages/monocytes displayed a non-inflammatory phenotype as judged by the low expression levels of (1) inflammasome components (including NLRP3, AIM2, and RIG-1) and (2) pro-inflammatory regulators (including IKKβ, RelA, TNFAIP3, and OPTN) at both protein (Figure 5C) and RNA (Figure 5D) levels compared with inflammatory BMDMs. This expression profile correlated with very low levels

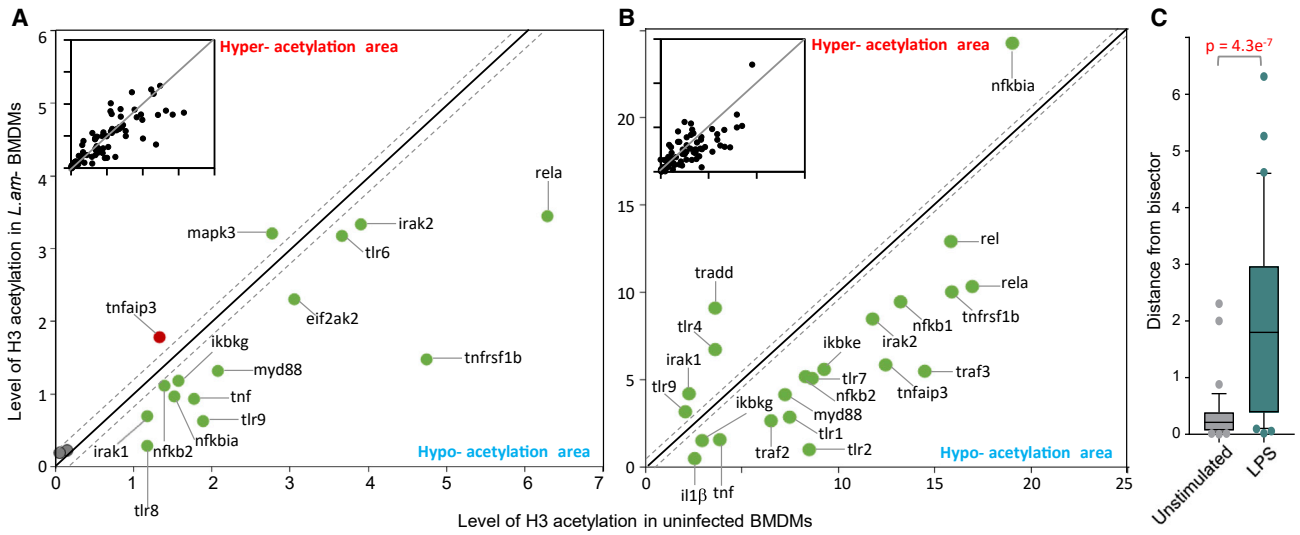

Figure 4. *L. am* Infection Modulates Macrophage H3 Acetylation at Promoters of NF-κB-Related Genes

Chromatin immunoprecipitation (ChIP) was performed on uninfected and *L. am*-infected BMDMs at 3 days PI, in the presence or absence of LPS. Following nuclei isolation, chromatin shearing, and immunoprecipitation with control and anti-histone H3 K9/K14 antibodies, qPCR assays were performed on chromatin preparations to measure enrichment of genomic DNA promoter sequence for genes associated with NF-κB signaling (EpiTect ChIP qPCR array, mouse NF-κB signaling pathway).

(A and B) Biparametric dot plots of the level of H3 acetylation in non-infected (x axis) and *L. am*-infected (y axis) BMDMs in absence (A; mean values of n = 2 independent experiments) or presence (B; n = 1 experiment) of LPS stimulation. The inserts show the results obtained for all gene promotors analyzed, while the main panels show the results for those gene for which abundance of their corresponding transcripts were analyzed previously by qRT-PCR (see Figure 3). The bisector is denoted by the diagonal black line. The unmodulated zone is comprised between the two dotted lines, which separate hypo- and hyper-acetylation zones. Green and red dots correspond to gene promoters associated with down- and up-modulated transcript abundance, respectively.

(C) Box-and-whisker plots representing the distribution of the distance between H3 acetylation levels of unstimulated (A) and LPS-treated (B) in *L. am*-infected BMDMs and the corresponding bisector. Distributions have been calculated for genes whose transcript abundance has been assessed by qRT-PCR.

of H3K9/14 acetylation at promoters of pro-inflammatory genes of the TLR-NF-κB-inflammasome axis compared with inflammatory or control BMDMs (Figures 5E and 5F). The low level of H3 activation marks extends to H3K4 trimethylation for the majority of analyzed promoters, with the exception of NLRP12, NF-kBia, and the anti-inflammatory regulator TOLLIP (Figure 5F, lower panel). Lesional macrophages failed to respond to LPS/ATP treatment and prevented priming and activation of inflammasomes, as shown by (1) the non-significant level of IL-1β secretion (Figure 5G) and (2) the absence or strongly reduced induction of inflammasome (NLRP3, NLRC4, AIM2, and RIG-1; Figure 5H) as well as of the NF-κB pathway (IKKβ, RelA, TNFAIP3, OPTN) components (Figure 5I). This unresponsiveness of lesional macrophages to LPS/ATP stimulation further extended to a very strong, global reduction in transcript abundance of 20 pro-inflammatory genes compared with BMDMs (Figure 5J), affecting the expression of various inflammasome components and positive as well as negative regulators of the NF-κB pathway (Figure 5K). Together these data validate the epigenetic and transcriptomic inhibition of the pro-inflammatory response in *L. am*-infected macrophages *in situ*.

DISCUSSION

Leishmania has evolved molecular strategies to harness the phenotypic potential of its macrophage host cell, often with devastating consequences for infected individuals (Gollob et al., 2014; Kaye and Scott, 2011). Using primary murine macrophages infected with lesion-derived *L. am* amastigotes and lesional monocytes/macrophages purified from infected mice, we demonstrate that this dominant human pathogen remodels the host cell chromatin during infection to establish permissive conditions for persistent intracellular survival (Figure 6). We show that the strong reduction of two distinct histone H3 activation marks (i.e., H3K9/K14 acetylation and H3K4 trimethylation) at host pro-inflammatory promoter genes correlates with decreased expression of crucial NF-κB and inflammasome activators. This finding reports a major mechanism underlying the strong anti-inflammatory and immune subversive properties *L. am* exerts on its host cell (de Freitas et al., 2016; Espitia et al., 2014; Kong et al., 2017; Liese et al., 2008; Soong, 2012; Stäger et al., 2010). Such anti-inflammatory properties are shared among all *Leishmania* species, and it is therefore interesting to speculate that the immunopathologies underlying the different forms of clinical leishmaniasis may have a common epigenetic root (Gollob et al., 2014; Soong et al., 2012), a possibility that remains to be tested.

During microbial infections, the macrophage phenotype is regulated in a highly dynamic manner by a combination of cell-specific transcription factors and chromatin modifications, which adapt the cell's transcriptional response to either promote or resolve inflammation (De Santa et al., 2009; Ehrt et al., 2001; Rolando et al., 2013). Various viral, prokaryotic, and eukaryotic microorganisms have evolved strategies to interfere with host cell

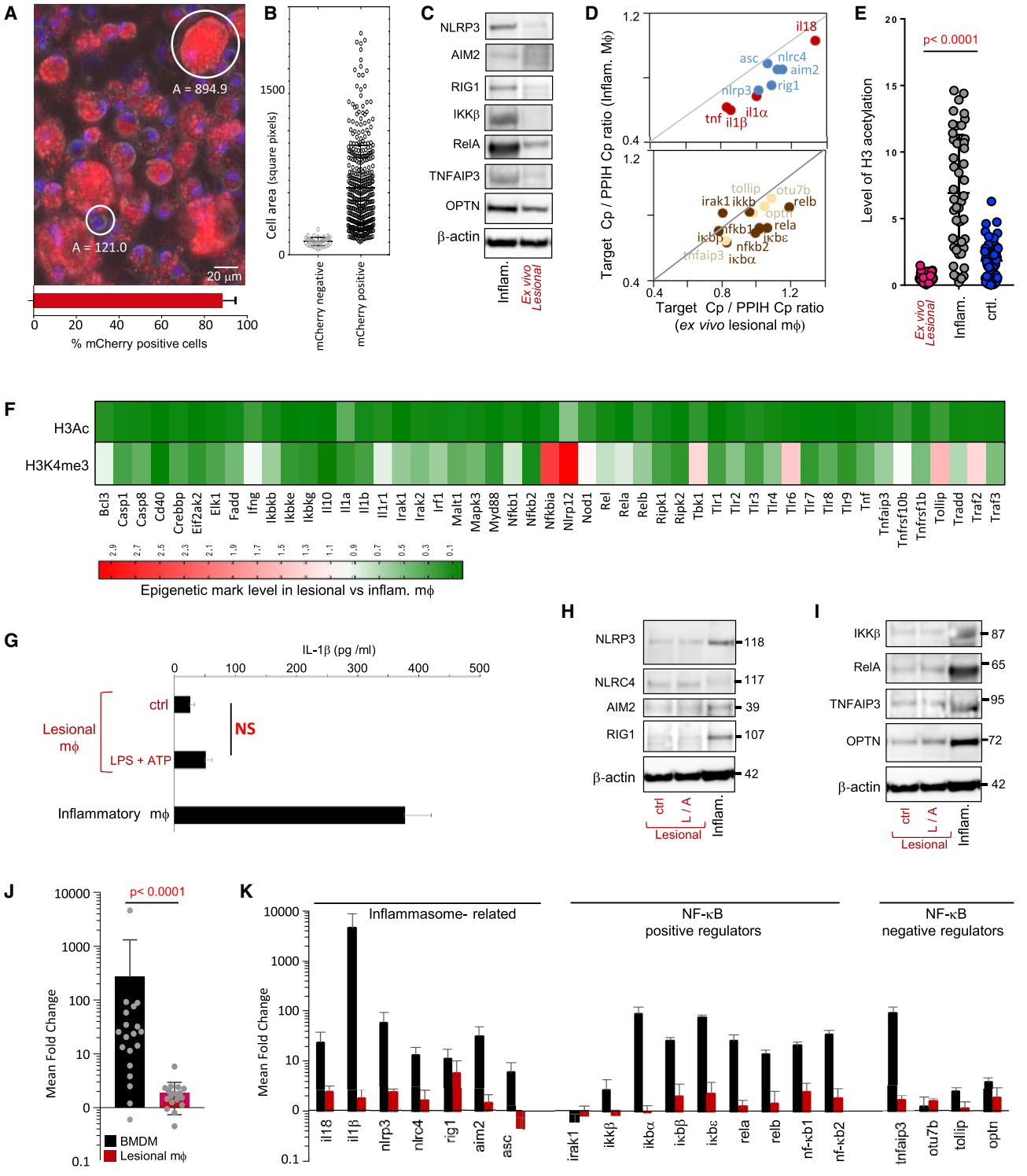

Figure 5. Transcriptomic and epigenetic inhibition of the pro-inflammatory response in *L. am*-infected, lesional macrophages

mCherry transgenic *L. am* parasites were inoculated into the footpads of BALB/c nude mice. Two months later, footpads were recovered to isolate lesional monocytes / macrophages.

(A and B) Epifluorescence microscopy analysis of *ex vivo* lesional monocytes / macrophages.

(A) Representative picture showing infected macrophages containing numerous amastigotes (mCherry, red). Cell nuclei were stained with Hoechst 33342 (blue). The area of one large, infected and one small, non-infected cell is indicated. The box plot shows the mean percentage of mCherry-positive cells in the lesion-derived cell population (mean ± SEM, n = 3 independent experiments).

(legend continued on next page)

transcriptional and epigenetic regulation (Cock-Rada et al., 2012; Ding et al., 2010; Hamon et al., 2007; Han et al., 2012; Hari Dass and Vyas, 2014; Kinnaird et al., 2013; Lang et al., 2012; Leng et al., 2009; Marazzi et al., 2012; Marr et al., 2014; Rolando et al., 2013). Our data provide first evidence that *Leishmania* adopts a similar strategy causing a fine-tuned, dichotomic dysregulation of the macrophage inflammatory response, characterized by concurrent suppression of pro-inflammatory and upregulation of anti-inflammatory components of the NF-κB signaling and NLRP3 inflammasome pathways on transcriptional and epigenetic levels. Surprisingly, de-activating of these two major components of the host anti-microbial response (Bauernfeind and Hornung, 2013; Evavold and Kagan, 2018; Liang et al., 2004; Próchnicki et al., 2016; Rahman and McFadden, 2011; Smale, 2011) was stage specific and observed only for disease-causing amastigotes, an important aspect that escaped a previous investigation of inflammasome activation in response to insect-stage promastigotes (Lima-Junior et al., 2013). In addition, *L. am* amastigotes prevent the priming of NLRP3 but also of other inflammasomes, such as RIG-1 and AIM2. To our knowledge, such a global subversion has not been shown for any other microbial infection. The absence of inflammasome priming documented here *in vitro* and *in vivo* likely explains the impaired IL-1β expression previously observed in lesions of *L. am*-infected mice, in particular during the first weeks PI (Ji et al., 2003). Abrogation of inflammasome priming *in vivo* likely has important consequences for parasite survival and anti-microbial immunity, given the role of NLRP3 activation and IL-1β secretion in restricting parasite load and lesion development (Lima-Junior et al., 2013). This may underlie the non-inflammatory, anergic diffuse form of leishmaniasis caused by *L. am* (Christensen et al., 2019; Scorza et al., 2017) in contrast to non-healing lesions that were associated with inflammasome activation (Charmoy et al., 2016; Gupta et al., 2019; Lee et al., 2018; Moreira et al., 2017).

Although the parasite effector mechanisms causing host cell immune suppression remain elusive and may involve various parasite- or host-derived signals, including anti-inflammatory cytokines such as IL-10 (Conaway et al., 2017), our study draws a detailed and complex picture of their impact on the host cell phenotype. We reveal a long-lasting (more than 3 weeks) and global inhibition of the NF-κB-mediated pro-inflammatory response on the transcriptomics level, which extends previous findings on specific inhibition of this pathway early during infection, involving cleavage of individual NF-κB members (Abu-Dayyeh et al., 2010; Calegari-Silva et al., 2009; Cameron et al., 2004; Gregory et al., 2008), the formation of Crel/P50 or P50/P50 dimers (Calegari-Silva et al., 2009; Guizani-Tabbane et al., 2004), the specific increase of key inhibitors of TLR signaling such as TNFAIP3 or IRAKm (Hartley et al., 2018; Srivastav et al., 2012, 2015), or the inhibition of TRAF3 degradation (Gupta et al., 2017). Thus, *L. am* not only avoids inflammasome activation early during infection, allowing the establishment of macrophage infection, but reprograms its host cell into a safe haven permissive for long-term, persistent infection and intracellular parasite growth. This phenotypic shift not only affects the host cells immune potential but may also cause the profound metabolic effects observed in *Leishmania*-infected macrophages (França-Costa et al., 2015; Osorio y Fortéa et al., 2009) that may feedback on the macrophage phenotype and its polarization state (Jaramillo et al., 2011; Martin et al., 2012).

Our findings showcase *Leishmania* as a pivotal model system to probe macrophage plasticity. The previously described *Leishmania*-induced metabolic re-tooling of the host cell directly supports the anti-inflammatory effect of parasite infection, likely through establishing a M2-like macrophage phenotype, a polarization profile known to be involved in the resolution of inflammation and characterized by upregulation of inhibitors of the NF-κB signaling pathway and the decreased expression of IL-1β, IL-18, and inflammasome components (Awad et al., 2017; Osorio y Fortéa et al., 2009). Understanding macrophage plasticity by using intracellular pathogens such as *Leishmania* and ultimately harnessing this process by pharmacological or immunological intervention opens exciting new venues for therapy. Our insights into *Leishmania* epigenetic, anti-inflammatory control can stimulate the development of new therapeutic options, for example, mimicking the parasite's suppressive effect on the NF-κB pathway, which is a major focus of curative intervention given its role in chronic inflammatory diseases (Durand and Baldwin, 2017; Herrington et al., 2016; Lin et al., 2017; Zeligs et al., 2016). Likewise, our findings open exciting new venues for host-directed, anti-leishmanial intervention strategies targeting the host cell epigenome, which has been recently proposed as

(B) Quantitation of the area of infected (mCherry positive) and non-infected (mCherry negative) cells in a representative, lesion-derived cell population (n = 430 cells).
(C–F) Comparative analysis of *ex vivo* lesional monocytes / macrophages and non-infected control (E) or pro-inflammatory, LPS/ATP-stimulated BMDMs (F).
(C) Western blot analysis of NLRP3, NLRC4, AIM-2 and RIG-1 inflammasomes in lysates of *ex vivo* lesional monocytes / macrophages and pro-inflammatory BMDMs.
(D) qRT-PCR analysis. Comparison of the ratio between the Crossing point (Cp) of the transcript of interest (target Cp) to the Cp of the reference gene (ppih) from *ex vivo* lesional vs pro-inflammatory macrophages. Comparisons are displayed for inflammasome components (blue) and cytokines (red) (left panel), and for NF-κB positive (dark brown) and negative (light brown) regulators (right panel).
(E) Comparison of the acetylation level of H3 in ctrl uninfected BMDMs and *ex vivo* lesional monocytes / macrophages ChIPqPCR. Chromatin immuno-precipitation was performed on inflammatory macrophages and in *ex vivo* lesional monocytes / macrophages with antibodies specific for acetylated H3K9/K14. qPCR assays were performed on chromatin preparations to measure enrichment of genomic DNA promoter sequence for genes associated with NF-κB signaling (EpiTect® ChIP qPCR Array, mouse NF-κB Signaling Pathway).
(F) Heat maps showing the ratio of the level of H3K9/K14 acetylation and H3K4 trimethylation in *ex vivo* lesional monocytes / macrophages vs inflammatory BMDMs.
(G–K) Comparative analysis of pro-inflammatory macrophages and lesional monocytes / macrophages stimulated with LPS/ATP after *ex vivo* isolation. (G) Detection by ELISA of secreted IL-1β in supernatants. Western blot analysis of inflammasome components (H) and members of the NF-κB pathway (I) in macrophage lysates. Note that the same loading control is shown in panels H and I as results were obtained using the same extracts. Global (J) and individual (K) transcriptional modulations of key components of the NF-κB – inflammasome axis (n = 20 targets, shown in (K) in response to LPS stimulation of BMDMs (black bars) and lesional monocytes / macrophages (red bars).

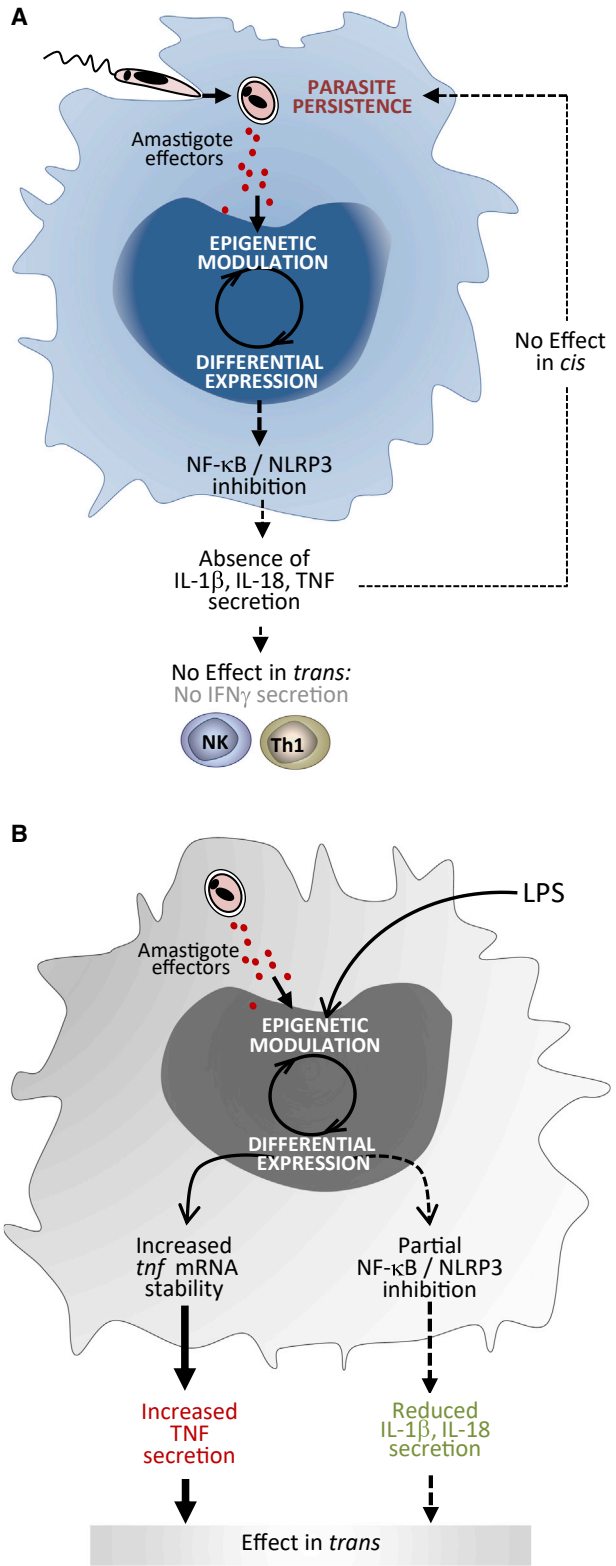

Figure 6. Models of the Subversion of the NF-κB-NLRP3 Immune Axis Induced by *L. am* Amastigotes in BALB/c BMDMs

(A) Under steady-state conditions, unknown amastigote-released effectors modulate the host cell epigenetic profile, likely causing the important changes in transcript abundance we observed for the genes of the NF-κB and NLRP3 signaling pathways. Absence of pro-inflammatory IL-1β, IL-18, and TNF production allows silent infection, undetected by non-infected bystander cells, thereby favoring the establishment of infection and early parasite survival.

(B) In the presence of bacterial products (i.e., LPS), the epigenetic effects caused by *Leishmania* amastigotes counteract those induced through TLRs and induce a paradoxical pattern of cytokine secretion, characterized by (1) increased TNF synthesis and secretion involving stabilization of the mRNA and (2) decreased IL-1β and IL-18 production, which correlates with the transcriptional inhibition of positive regulators of the NF-κB and NLRP3 axes.

a promising way to guard against the selection of drug resistant parasites (Afrin et al., 2019; Kumar et al., 2017; Lamotte et al., 2017; Prieto Barja et al., 2017).

In conclusion, we provide evidence for remodeling of the macrophage chromatin during *Leishmania* infection that affects the host cells' immune effector functions and metabolism, establishing permissive conditions for intracellular parasite survival. Whether the *Leishmania*-induced changes in the host cell epigenome are a cause or consequence of the observed phenotypic response remains to be elucidated. However, the correlation we observed between histone H3K9/K14 hypoacetylation and H3K4 hypomethylation and transcriptional downregulation for pro-inflammatory surface receptors (TLR4, TNFR), signaling molecules (MYD88, RIPK2), transcription factors (RelA, RelB, NF-κB1, NF-κB2), and cytokines (IL-1β, TNF) suggests that chromatin remodeling is the cause of the macrophage phenotypic change. Modulation of H3 modification itself may be transcriptionally regulated, as suggested by previous transcriptomics analyses that revealed changes in HDAC expression in *L. am*-infected BMDMs (Calegari-Silva et al., 2018; Osorio y Fortéa et al., 2009). Likewise, the release of parasite histones (Silverman et al., 2010) may alter host H3 modification through competition with host HMEs, and host histones may be directly modified by parasite HMEs, such as SIRTUIN 2 (Ronin et al., 2018; Tavares et al., 2010; Yahiaoui et al., 1996) or various histone acetyltransferases (Chandra et al., 2017; Kumar et al., 2012; Kumar and Saha, 2015; Maity and Saha, 2012). Future studies investigating macrophage-*Leishmania* interactions at the systems level combining transcriptomic, epigenetic, and metabolomic analyses will shed new light on the mechanisms underlying host cell chromatin remodeling, with the potential to uncover new candidates for host-directed, anti-leishmanial therapy.

STAR★METHODS

Detailed methods are provided in the online version of this paper and include the following:

- KEY RESOURCES TABLE
- LEAD CONTACT AND MATERIALS AVAILABILITY
- EXPERIMENTAL MODEL AND SUBJECT DETAILS
  - Ethics Statement
  - Isolation and Culture of Bone-Marrow-Derived Macrophages
  - Inflammasome Activation in Macrophage Cultures
  - Parasite Isolation and BMDM Infection
  - Generation of *Ex Vivo* Macrophages in BALB/c Nude Mice

SUPPLEMENTAL INFORMATION

Supplemental Information can be found online at https://doi.org/10.1016/j.celrep.2020.01.030.

ACKNOWLEDGMENTS

This project was supported by a fund of the Institut Pasteur International Direction to the International Mixed Unit "Inflammation and Leishmania Infection" and by the International Partnership Program (153831KYSB20190008) of the Chinese Academy of Sciences. We would like to thank Jean-Marc Cavaillon for support and helpful discussions and Drs. Emmanuel Laplantine and Anastassia V. Komarova for providing antibodies. The UtechS PBI/C2RT is part of the FranceBioImaging infrastructure, supported by the French National Research Agency (ANR-10-INSB-04-01, Investments for the Future) and is supported by Conseil de la Région Ile-de-France (Domaine d'Intérêt Majeur DIM1HEALTH) and Fondation Française pour la Recherche Médicale (Programme Grands Equipements).

AUTHOR CONTRIBUTIONS

H.L., E.P., T.R., K.K., P.N., and Y.X. performed research. H.L., E.P., T.R., K.K., P.N., Y.X., N.A., H.V., and G.B. analyzed data. G. Milon and R.W. participated in scientific discussions. R.W. provided personal reagents. H.L., E.P., G. Meng, and G.F.S. designed research and wrote the paper. All authors read and approved the final manuscript.

DECLARATION OF INTERESTS

The authors declare no competing interests.

Received: September 14, 2018
Revised: November 8, 2019
Accepted: January 8, 2020
Published: February 11, 2020

REFERENCES

Abu-Dayyeh, I., Hassani, K., Westra, E.R., Mottram, J.C., and Olivier, M. (2010). Comparative study of the ability of *Leishmania mexicana* promastigotes and amastigotes to alter macrophage signaling and functions. Infect. Immun. *78*, 2438–2445.

Afrin, F., Khan, I., and Hemeg, H.A. (2019). *Leishmania*-host interactions—an epigenetic paradigm. Front. Immunol. *10*, 492.

Alvar, J., Vélez, I.D., Bern, C., Herrero, M., Desjeux, P., Cano, J., Jannin, J., and den Boer, M.; WHO Leishmaniasis Control Team (2012). Leishmaniasis worldwide and global estimates of its incidence. PLoS ONE *7*, e35671.

Antoine, J.C., Prina, E., Lang, T., and Courret, N. (1998). The biogenesis and properties of the parasitophorous vacuoles that harbour *Leishmania* in murine macrophages. Trends Microbiol. *6*, 392–401.

Arango Duque, G., and Descoteaux, A. (2015). *Leishmania* survival in the macrophage: where the ends justify the means. Curr. Opin. Microbiol. *26*, 32–40.

Arrigoni, L., Richter, A.S., Betancourt, E., Bruder, K., Diehl, S., Manke, T., and Bönisch, U. (2016). Standardizing chromatin research: a simple and universal method for ChIP-seq. Nucleic Acids Res. *44*, e67.

Awad, F., Assrawi, E., Jumeau, C., Georgin-Lavialle, S., Cobret, L., Duquesnoy, P., Piterboth, W., Thomas, L., Stankovic-Stojanovic, K., Louvrier, C., et al. (2017). Impact of human monocyte and macrophage polarization on NLR expression and NLRP3 inflammasome activation. PLoS ONE *12*, e0175336.

Bauernfeind, F., and Hornung, V. (2013). Of inflammasomes and pathogens–sensing of microbes by the inflammasome. EMBO Mol. Med. *5*, 814–826.

Bellamy, R. (1999). The natural resistance-associated macrophage protein and susceptibility to intracellular pathogens. Microbes Infect. *1*, 23–27.

Benoit, M., Desnues, B., and Mege, J.L. (2008). Macrophage polarization in bacterial infections. J. Immunol. *181*, 3733–3739.

Biswas, S.K., and Mantovani, A. (2010). Macrophage plasticity and interaction with lymphocyte subsets: cancer as a paradigm. Nat. Immunol. *11*, 889–896.

Calegari-Silva, T.C., Pereira, R.M., De-Melo, L.D., Saraiva, E.M., Soares, D.C., Bellio, M., and Lopes, U.G. (2009). NF-kappaB-mediated repression of iNOS expression in *Leishmania amazonensis* macrophage infection. Immunol. Lett. *127*, 19–26.

Calegari-Silva, T.C., Vivarini, A.C., Pereira, R.M.S., Dias-Teixeira, K.L., Rath, C.T., Pacheco, A.S.S., Silva, G.B.L., Pinto, C.A.S., Dos Santos, J.V., Saliba, A.M., et al. (2018). Leishmania amazonensis downregulates macrophage iNOS expression via Histone Deacetylase 1 (HDAC1): a novel parasite evasion mechanism. Eur. J. Immunol. *48*, 1188–1198.

Cameron, P., McGachy, A., Anderson, M., Paul, A., Coombs, G.H., Mottram, J.C., Alexander, J., and Plevin, R. (2004). Inhibition of lipopolysaccharide-induced macrophage IL-12 production by *Leishmania mexicana* amastigotes: the role of cysteine peptidases and the NF-kappaB signaling pathway. J. Immunol. *173*, 3297–3304.

Canonne-Hergaux, F., Gruenheid, S., Govoni, G., and Gros, P. (1999). The Nramp1 protein and its role in resistance to infection and macrophage function. Proc. Assoc. Am. Physicians *111*, 283–289.

Chandra, U., Yadav, A., Kumar, D., and Saha, S. (2017). Cell cycle stage-specific transcriptional activation of cyclins mediated by HAT2-dependent H4K10 acetylation of promoters in Leishmania donovani. PLoS Pathog. *13*, e1006615.

Charmoy, M., Hurrell, B.P., Romano, A., Lee, S.H., Ribeiro-Gomes, F., Riteau, N., Mayer-Barber, K., Tacchini-Cottier, F., and Sacks, D.L. (2016). The Nlrp3 inflammasome, IL-1β, and neutrophil recruitment are required for susceptibility to a nonhealing strain of Leishmania major in C57BL/6 mice. Eur. J. Immunol. *46*, 897–911.

Christensen, S.M., Belew, A.T., El-Sayed, N.M., Tafuri, W.L., Silveira, F.T., and Mosser, D.M. (2019). Host and parasite responses in human diffuse cutaneous leishmaniasis caused by L. amazonensis. PLoS Negl. Trop. Dis. *13*, e0007152.

Cock-Rada, A.M., Medjkane, S., Janski, N., Yousfi, N., Perichon, M., Chaussepied, M., Chluba, J., Langsley, G., and Weitzman, J.B. (2012). SMYD3 promotes cancer invasion by epigenetic upregulation of the metalloproteinase MMP-9. Cancer Res. *72*, 810–820.

Conaway, E.A., de Oliveira, D.C., McInnis, C.M., Snapper, S.B., and Horwitz, B.H. (2017). Inhibition of inflammatory gene transcription by IL-10 is associated with rapid suppression of lipopolysaccharide-induced enhancer activation. J. Immunol. *198*, 2906–2915.

de Freitas, E.O., Leoratti, F.M., Freire-de-Lima, C.G., Morrot, A., and Feijó, D.F. (2016). The contribution of immune evasive mechanisms to parasite persistence in visceral leishmaniasis. Front. Immunol. *7*, 153.

de La Llave, E., Lecoeur, H., Besse, A., Milon, G., Prina, E., and Lang, T. (2011). A combined luciferase imaging and reverse transcription polymerase chain reaction assay for the study of Leishmania amastigote burden and correlated mouse tissue transcript fluctuations. Cell. Microbiol. *13*, 81–91.

De Santa, F., Narang, V., Yap, Z.H., Tusi, B.K., Burgold, T., Austenaa, L., Bucci, G., Caganova, M., Notarbartolo, S., Casola, S., et al. (2009). Jmjd3 contributes to the control of gene expression in LPS-activated macrophages. EMBO J. *28*, 3341–3352.

Dey, R., Joshi, A.B., Oliveira, F., Pereira, L., Guimaraes-Costa, A.B., Serafim, T.D., de Castro, W., Coutinho-Abreu, I.V., Bhattacharya, P., Townsend, S., et al. (2018). Gut microbes egested during bites of infected sand flies augment severity of leishmaniasis via inflammasome-derived IL-1beta. Cell Host Microbe *23*, 134–143.e6.

Ding, S.Z., Fischer, W., Kaparakis-Liaskos, M., Liechti, G., Merrell, D.S., Grant, P.A., Ferrero, R.L., Crowe, S.E., Haas, R., Hatakeyama, M., and Goldberg, J.B. (2010). *Helicobacter pylori*-induced histone modification, associated gene expression in gastric epithelial cells, and its implication in pathogenesis. PLoS ONE *5*, e9875.

Durand, J.K., and Baldwin, A.S. (2017). Targeting IKK and NF-κB for therapy. Adv. Protein Chem. Struct. Biol. *107*, 77–115.

Ehrt, S., Schnappinger, D., Bekiranov, S., Drenkow, J., Shi, S., Gingeras, T.R., Gaasterland, T., Schoolnik, G., and Nathan, C. (2001). Reprogramming of the macrophage transcriptome in response to interferon-gamma and *Mycobacterium tuberculosis*: signaling roles of nitric oxide synthase-2 and phagocyte oxidase. J. Exp. Med. *194*, 1123–1140.

Espitia, C.M., Saldarriaga, O.A., Travi, B.L., Osorio, E.Y., Hernandez, A., Band, M., Patel, M.J., Medina, A.A., Cappello, M., Pekosz, A., and Melby, P.C. (2014). Transcriptional profiling of the spleen in progressive visceral leishmaniasis reveals mixed expression of type 1 and type 2 cytokine-responsive genes. BMC Immunol. *15*, 38.

Evavold, C.L., and Kagan, J.C. (2018). How inflammasomes inform adaptive immunity. J. Mol. Biol. *430*, 217–237.

Falvo, J.V., Tsytsykova, A.V., and Goldfeld, A.E. (2010). Transcriptional control of the TNF gene. Curr. Dir. Autoimmun. *11*, 27–60.

França-Costa, J., Van Weyenbergh, J., Boaventura, V.S., Luz, N.F., Malta-Santos, H., Oliveira, M.C., Santos de Campos, D.C., Saldanha, A.C., dos-Santos, W.L., Bozza, P.T., et al. (2015). Arginase I, polyamine, and prostaglandin E2 pathways suppress the inflammatory response and contribute to diffuse cutaneous leishmaniasis. J. Infect. Dis. *211*, 426–435.

Franchi, L., Muñoz-Planillo, R., and Núñez, G. (2012). Sensing and reacting to microbes through the inflammasomes. Nat. Immunol. *13*, 325–332.

Gazzinelli, R.T., Kalantari, P., Fitzgerald, K.A., and Golenbock, D.T. (2014). Innate sensing of malaria parasites. Nat. Rev. Immunol. *14*, 744–757.

Ghizzoni, M., Haisma, H.J., Maarsingh, H., and Dekker, F.J. (2011). Histone acetyltransferases are crucial regulators in NF-κB mediated inflammation. Drug Discov. Today *16*, 504–511.

Ginhoux, F., and Jung, S. (2014). Monocytes and macrophages: developmental pathways and tissue homeostasis. Nat. Rev. Immunol. *14*, 392–404.

Giraud, E., Lecoeur, H., Soubigou, G., Coppée, J.Y., Milon, G., Prina, E., and Lang, T. (2012). Distinct transcriptional signatures of bone marrow-derived C57BL/6 and DBA/2 dendritic leucocytes hosting live *Leishmania amazonensis* amastigotes. PLoS Negl. Trop. Dis. *6*, e1980.

Gollob, K.J., Viana, A.G., and Dutra, W.O. (2014). Immunoregulation in human American leishmaniasis: balancing pathology and protection. Parasite Immunol. *36*, 367–376.

Gordon, S., and Martinez, F.O. (2010). Alternative activation of macrophages: mechanism and functions. Immunity *32*, 593–604.

Gordon, S., and Taylor, P.R. (2005). Monocyte and macrophage heterogeneity. Nat. Rev. Immunol. *5*, 953–964.

Gregory, D.J., Godbout, M., Contreras, I., Forget, G., and Olivier, M. (2008). A novel form of NF-kappaB is induced by *Leishmania* infection: involvement in macrophage gene expression. Eur. J. Immunol. *38*, 1071–1081.

Guizani-Tabbane, L., Ben-Aissa, K., Belghith, M., Sassi, A., and Dellagi, K. (2004). *Leishmania major* amastigotes induce p50/c-Rel NF-kappa B transcription factor in human macrophages: involvement in cytokine synthesis. Infect. Immun. *72*, 2582–2589.

Gupta, A.K., Ghosh, K., Palit, S., Barua, J., Das, P.K., and Ukil, A. (2017). Leishmania donovani inhibits inflammasome-dependent macrophage activation by exploiting the negative regulatory proteins A20 and UCP2. FASEB J. *31*, 5087–5101.

Gupta, G., Santana, A.K.M., Gomes, C.M., Turatti, A., Milanezi, C.M., Bueno Filho, R., Fuzo, C., Almeida, R.P., Carregaro, V., Roselino, A.M., and Silva, J.S. (2019). Inflammasome gene expression is associated with immunopathology in human localized cutaneous leishmaniasis. Cell. Immunol. *341*, 103920.

Gurung, P., Karki, R., Vogel, P., Watanabe, M., Bix, M., Lamkanfi, M., and Kanneganti, T.D. (2015). An NLRP3 inflammasome-triggered Th2-biased adaptive immune response promotes leishmaniasis. J. Clin. Invest. *125*, 1329–1338.

Hamon, M.A., Batsché, E., Régnault, B., Tham, T.N., Seveau, S., Muchardt, C., and Cossart, P. (2007). Histone modifications induced by a family of bacterial toxins. Proc. Natl. Acad. Sci. U S A *104*, 13467–13472.

Han, X., Li, X., Yue, S.C., Anandaiah, A., Hashem, F., Reinach, P.S., Koziel, H., and Tachado, S.D. (2012). Epigenetic regulation of tumor necrosis factor α (TNFα) release in human macrophages by HIV-1 single-stranded RNA (ssRNA) is dependent on TLR8 signaling. J. Biol. Chem. *287*, 13778–13786.

Hari Dass, S.A., and Vyas, A. (2014). *Toxoplasma gondii* infection reduces predator aversion in rats through epigenetic modulation in the host medial amygdala. Mol. Ecol. *23*, 6114–6122.

Hartley, M.A., Eren, R.O., Rossi, M., Prevel, F., Castiglioni, P., Isorce, N., Desponds, C., Lye, L.F., Beverley, S.M., Drexler, S.K., and Fasel, N. (2018). *Leishmania guyanensis* parasites block the activation of the inflammasome by inhibiting maturation of IL-1β. Microb. Cell *5*, 137–149.

He, Y., Hara, H., and Núñez, G. (2016). Mechanism and regulation of NLRP3 inflammasome activation. Trends Biochem. Sci. *41*, 1012–1021.

Herbein, G., and Varin, A. (2010). The macrophage in HIV-1 infection: from activation to deactivation? Retrovirology *7*, 33.

Herbert, D.R., Hölscher, C., Mohrs, M., Arendse, B., Schwegmann, A., Radwanska, M., Leeto, M., Kirsch, R., Hall, P., Mossmann, H., et al. (2004). Alternative macrophage activation is essential for survival during schistosomiasis and downmodulates T helper 1 responses and immunopathology. Immunity *20*, 623–635.

Herrington, F.D., Carmody, R.J., and Goodyear, C.S. (2016). Modulation of NF-κB signaling as a therapeutic target in autoimmunity. J. Biomol. Screen. *21*, 223–242.

Jaramillo, M., Gomez, M.A., Larsson, O., Shio, M.T., Topisirovic, I., Contreras, I., Luxenburg, R., Rosenfeld, A., Colina, R., McMaster, R.W., et al. (2011). *Leishmania* repression of host translation through mTOR cleavage is required for parasite survival and infection. Cell Host Microbe *9*, 331–341.

Ji, J., Sun, J., and Soong, L. (2003). Impaired expression of inflammatory cytokines and chemokines at early stages of infection with *Leishmania amazonensis*. Infect. Immun. *71*, 4278–4288.

Jo, E.K., Kim, J.K., Shin, D.M., and Sasakawa, C. (2016). Molecular mechanisms regulating NLRP3 inflammasome activation. Cell. Mol. Immunol. *13*, 148–159.

Kapellos, T.S., and Iqbal, A.J. (2016). Epigenetic control of macrophage polarisation and soluble mediator gene expression during inflammation. Mediators Inflamm. *2016*, 6591703.

Kaye, P., and Scott, P. (2011). Leishmaniasis: complexity at the host-pathogen interface. Nat. Rev. Microbiol. *9*, 604–615.

Kinnaird, J.H., Weir, W., Durrani, Z., Pillai, S.S., Baird, M., and Shiels, B.R. (2013). A bovine lymphosarcoma cell line infected with *Theileria annulata* exhibits an irreversible reconfiguration of host cell gene expression. PLoS ONE *8*, e66833.

Kong, F., Saldarriaga, O.A., Spratt, H., Osorio, E.Y., Travi, B.L., Luxon, B.A., and Melby, P.C. (2017). Transcriptional profiling in experimental visceral leishmaniasis reveals a broad splenic inflammatory environment that conditions macrophages toward a disease-promoting phenotype. PLoS Pathog. *13*, e1006165.

Kumar, D., and Saha, S. (2015). HAT3-mediated acetylation of PCNA precedes PCNA monoubiquitination following exposure to UV radiation in Leishmania donovani. Nucleic Acids Res. *43*, 5423–5441.

Kumar, D., Rajanala, K., Minocha, N., and Saha, S. (2012). Histone H4 lysine 14 acetylation in Leishmania donovani is mediated by the MYST-family protein HAT4. Microbiology *158*, 328–337.

Kumar, R., Chauhan, S.B., Ng, S.S., Sundar, S., and Engwerda, C.R. (2017). Immune checkpoint targets for host-directed therapy to prevent and treat leishmaniasis. Front. Immunol. *8*, 1492.

Lamotte, S., Späth, G.F., Rachidi, N., and Prina, E. (2017). The enemy within: targeting host-parasite interaction for antileishmanial drug discovery. PLoS Negl. Trop. Dis. *11*, e0005480.

Lang, C., Hildebrandt, A., Brand, F., Opitz, L., Dihazi, H., and Lüder, C.G. (2012). Impaired chromatin remodelling at STAT1-regulated promoters leads to global unresponsiveness of Toxoplasma gondii-infected macrophages to IFN-γ. PLoS Pathog. *8*, e1002483.

Lecoeur, H., de La Llave, E., Osorio Y Fortéa, J., Goyard, S., Kiefer-Biasizzo, H., Balazuc, A.M., Milon, G., Prina, E., and Lang, T. (2010). Sorting of *Leishmania*-bearing dendritic cells reveals subtle parasite-induced modulation of host-cell gene expression. Microbes Infect. *12*, 46–54.

Lecoeur, H., Giraud, E., Prévost, M.C., Milon, G., and Lang, T. (2013). Reprogramming neutral lipid metabolism in mouse dendritic leucocytes hosting live *Leishmania amazonensis* amastigotes. PLoS Negl. Trop. Dis. *7*, e2276.

Lee, S.H., Charmoy, M., Romano, A., Paun, A., Chaves, M.M., Cope, F.O., Ralph, D.A., and Sacks, D.L. (2018). Mannose receptor high, M2 dermal macrophages mediate nonhealing *Leishmania major* infection in a Th1 immune environment. J. Exp. Med. *215*, 357–375.

Leng, J., Butcher, B.A., Egan, C.E., Abi Abdallah, D.S., and Denkers, E.Y. (2009). *Toxoplasma gondii* prevents chromatin remodeling initiated by TLR-triggered macrophage activation. J. Immunol. *182*, 489–497.

Liang, Y., Zhou, Y., and Shen, P. (2004). NF-kappaB and its regulation on the immune system. Cell. Mol. Immunol. *1*, 343–350.

Liese, J., Schleicher, U., and Bogdan, C. (2008). The innate immune response against *Leishmania* parasites. Immunobiology *213*, 377–387.

Lima-Junior, D.S., Costa, D.L., Carregaro, V., Cunha, L.D., Silva, A.L., Mineo, T.W., Gutierrez, F.R., Bellio, M., Bortoluci, K.R., Flavell, R.A., et al. (2013). Inflammasome-derived IL-1β production induces nitric oxide-mediated resistance to Leishmania. Nat. Med. *19*, 909–915.

Lin, T.H., Pajarinen, J., Lu, L., Nabeshima, A., Cordova, L.A., Yao, Z., and Goodman, S.B. (2017). NF-κB as a Therapeutic Target in Inflammatory-Associated Bone Diseases. Adv. Protein Chem. Struct. Biol. *107*, 117–154.

Maity, A.K., and Saha, P. (2012). The histone acetyl transferase LdHAT1 from Leishmania donovani is regulated by S-phase cell cycle kinase. FEMS Microbiol. Lett. *336*, 57–63.

Marazzi, I., Ho, J.S., Kim, J., Manicassamy, B., Dewell, S., Albrecht, R.A., Seibert, C.W., Schaefer, U., Jeffrey, K.L., Prinjha, R.K., et al. (2012). Suppression of the antiviral response by an influenza histone mimic. Nature *483*, 428–433.

Marr, A.K., MacIsaac, J.L., Jiang, R., Airo, A.M., Kobor, M.S., and McMaster, W.R. (2014). *Leishmania donovani* infection causes distinct epigenetic DNA methylation changes in host macrophages. PLoS Pathog. *10*, e1004419.

Martin, S., Saha, B., and Riley, J.L. (2012). The battle over mTOR: an emerging theatre in host-pathogen immunity. PLoS Pathog. *8*, e1002894.

McConville, M.J., Saunders, E.C., Kloehn, J., and Dagley, M.J. (2015). Leishmania carbon metabolism in the macrophage phagolysosome—feast or famine? F1000Res. *4* (*F1000 Faculty Rev*), 938.

Moreira, R.B., Pirmez, C., de Oliveira-Neto, M.P., Aguiar, L.S., Gonçalves, A.J.S., Pereira, L.O.R., Abreu, L., and De Oliveira, M.P. (2017). AIM2 inflammasome is associated with disease severity in tegumentary leishmaniasis caused by Leishmania (V.) braziliensis. Parasite Immunol. *39*, e12435.

Murray, P.J., Allen, J.E., Biswas, S.K., Fisher, E.A., Gilroy, D.W., Goerdt, S., Gordon, S., Hamilton, J.A., Ivashkiv, L.B., Lawrence, T., et al. (2014). Macrophage activation and polarization: nomenclature and experimental guidelines. Immunity *41*, 14–20.

Noël, W., Raes, G., Hassanzadeh Ghassabeh, G., De Baetselier, P., and Beschin, A. (2004). Alternatively activated macrophages during parasite infections. Trends Parasitol. *20*, 126–133.

Olivier, M., Gregory, D.J., and Forget, G. (2005). Subversion mechanisms by which *Leishmania* parasites can escape the host immune response: a signaling point of view. Clin. Microbiol. Rev. *18*, 293–305.

Osorio y Fortéa, J., Prina, E., de La Llave, E., Lecoeur, H., Lang, T., and Milon, G. (2007). Unveiling pathways used by *Leishmania amazonensis* amastigotes to subvert macrophage function. Immunol. Rev. *219*, 66–74.

Osorio y Fortéa, J., de La Llave, E., Regnault, B., Coppée, J.Y., Milon, G., Lang, T., and Prina, E. (2009). Transcriptional signatures of BALB/c mouse macrophages housing multiplying *Leishmania amazonensis* amastigotes. BMC Genomics *10*, 119.

Pathak, S.K., Basu, S., Basu, K.K., Banerjee, A., Pathak, S., Bhattacharyya, A., Kaisho, T., Kundu, M., and Basu, J. (2007). Direct extracellular interaction between the early secreted antigen ESAT-6 of *Mycobacterium tuberculosis* and TLR2 inhibits TLR signaling in macrophages. Nat. Immunol. *8*, 610–618.

Pearce, E.J., and MacDonald, A.S. (2002). The immunobiology of schistosomiasis. Nat. Rev. Immunol. *2*, 499–511.

Pfaffl, M.W., Horgan, G.W., and Dempfle, L. (2002). Relative expression software tool (REST) for group-wise comparison and statistical analysis of relative expression results in real-time PCR. Nucleic Acids Res. *30*, e36.

Prieto Barja, P., Pescher, P., Bussotti, G., Dumetz, F., Imamura, H., Kedra, D., Domagalska, M., Chaumeau, V., Himmelbauer, H., Pages, M., et al. (2017). Haplotype selection as an adaptive mechanism in the protozoan pathogen *Leishmania donovani*. Nat. Ecol. Evol. *1*, 1961–1969.

Prina, E., Abdi, S.Z., Lebastard, M., Perret, E., Winter, N., and Antoine, J.C. (2004). Dendritic cells as host cells for the promastigote and amastigote stages of *Leishmania amazonensis*: the role of opsonins in parasite uptake and dendritic cell maturation. J. Cell Sci. *117*, 315–325.

Próchnicki, T., Mangan, M.S., and Latz, E. (2016). Recent insights into the molecular mechanisms of the NLRP3 inflammasome activation. F1000Res. *5*, F1000 Faculty Rev-146.

Pujari, R., Hunte, R., Khan, W.N., and Shembade, N. (2013). A20-mediated negative regulation of canonical NF-κB signaling pathway. Immunol. Res. *57*, 166–171.

Raes, G., Beschin, A., Ghassabeh, G.H., and De Baetselier, P. (2007). Alternatively activated macrophages in protozoan infections. Curr. Opin. Immunol. *19*, 454–459.

Rahman, M.M., and McFadden, G. (2011). Modulation of NF-κB signalling by microbial pathogens. Nat. Rev. Microbiol. *9*, 291–306.

Renner, F., and Schmitz, M.L. (2009). Autoregulatory feedback loops terminating the NF-kappaB response. Trends Biochem. Sci. *34*, 128–135.

Rolando, M., Sanulli, S., Rusniok, C., Gomez-Valero, L., Bertholet, C., Sahr, T., Margueron, R., and Buchrieser, C. (2013). *Legionella pneumophila* effector RomA uniquely modifies host chromatin to repress gene expression and promote intracellular bacterial replication. Cell Host Microbe *13*, 395–405.

Ronin, C., Costa, D.M., Tavares, J., Faria, J., Ciesielski, F., Ciapetti, P., Smith, T.K., MacDougall, J., Cordeiro-da-Silva, A., and Pemberton, I.K. (2018). The crystal structure of the Leishmania infantum Silent Information Regulator 2 related protein 1: implications to protein function and drug design. PLoS ONE *13*, e0193602.

Sacks, D., and Noben-Trauth, N. (2002). The immunology of susceptibility and resistance to *Leishmania major* in mice. Nat. Rev. Immunol. *2*, 845–858.

Saeed, S., Quintin, J., Kerstens, H.H., Rao, N.A., Aghajanirefah, A., Matarese, F., Cheng, S.C., Ratter, J., Berentsen, K., van der Ent, M.A., et al. (2014). Epigenetic programming of monocyte-to-macrophage differentiation and trained innate immunity. Science *345*, 1251086.

Scorza, B.M., Carvalho, E.M., and Wilson, M.E. (2017). Cutaneous manifestations of human and murine leishmaniasis. Int. J. Mol. Sci. *18*, E1296.

Scott, P.A., and Farrell, J.P. (1981). Experimental cutaneous leishmaniasis. I. Nonspecific immunodepression in BALB/c mice infected with *Leishmania tropica*. J. Immunol. *127*, 2395–2400.

Scott, P.A., and Farrell, J.P. (1982). Experimental cutaneous leishmaniasis: disseminated leishmaniasis in genetically susceptible and resistant mice. Am. J. Trop. Med. Hyg. *31*, 230–238.

Silverman, J.M., Clos, J., de'Oliveira, C.C., Shirvani, O., Fang, Y., Wang, C., Foster, L.J., and Reiner, N.E. (2010). An exosome-based secretion pathway is responsible for protein export from *Leishmania* and communication with macrophages. J. Cell Sci. *123*, 842–852.

Smale, S.T. (2011). Hierarchies of NF-κB target-gene regulation. Nat. Immunol. *12*, 689–694.

Soong, L. (2012). Subversion and utilization of host innate defense by *Leishmania amazonensis*. Front. Immunol. *3*, 58.

Soong, L., Henard, C.A., and Melby, P.C. (2012). Immunopathogenesis of non-healing American cutaneous leishmaniasis and progressive visceral leishmaniasis. Semin. Immunopathol. *34*, 735–751.

Späth, G.F., and Beverley, S.M. (2001). A lipophosphoglycan-independent method for isolation of infective *Leishmania* metacyclic promastigotes by density gradient centrifugation. Exp. Parasitol. *99*, 97–103.

Srivastav, S., Kar, S., Chande, A.G., Mukhopadhyaya, R., and Das, P.K. (2012). *Leishmania donovani* exploits host deubiquitinating enzyme A20, a negative regulator of TLR signaling, to subvert host immune response. J. Immunol. *189*, 924–934.

Srivastav, S., Saha, A., Barua, J., Ukil, A., and Das, P.K. (2015). IRAK-M regulates the inhibition of TLR-mediated macrophage immune response during late in vitro *Leishmania donovani* infection. Eur. J. Immunol. *45*, 2787–2797.

Stäger, S., Joshi, T., and Bankoti, R. (2010). Immune evasive mechanisms contributing to persistent *Leishmania donovani* infection. Immunol. Res. *47*, 14–24.

Tavares, J., Ouaissi, A., Kong Thoo Lin, P., Loureiro, I., Kaur, S., Roy, N., and Cordeiro-da-Silva, A. (2010). Bisnaphthalimidopropyl derivatives as inhibitors of Leishmania SIR2 related protein 1. ChemMedChem *5*, 140–147.

Yahiaoui, B., Taibi, A., and Ouaissi, A. (1996). A Leishmania major protein with extensive homology to silent information regulator 2 of Saccharomyces cerevisiae. Gene *169*, 115–118.

Zeligs, K.P., Neuman, M.K., and Annunziata, C.M. (2016). Molecular pathways: the balance between cancer and the immune system challenges the therapeutic specificity of targeting nuclear factor-kappaB signaling for cancer treatment. Clin. Cancer Res. *22*, 4302–4308.

Zilberstein, D., and Shapira, M. (1994). The role of pH and temperature in the development of *Leishmania* parasites. Annu. Rev. Microbiol. *48*, 449–470.

STAR★METHODS

KEY RESOURCES TABLE

REAGENT or RESOURCE	SOURCE	IDENTIFIER
Antibodies		
Mouse monoclonal anti-IkBβ	Abgent	Cat#AM8109a, 62AT216 clone; RRID:AB_2233422
Rabbit polyclonal anti-IKKγ	Santa Cruz Biotechnology	Cat#sc-8330; RRID:AB_2124846
Rabbit monoclonal anti- P-IkBα	ThermoFisher scientific	Cat#MA5-14857; J10.3 clone, lot QE2031854; RRID:AB_10986824
Rabbit monoclonal anti- IkBα	Abcam	Cat#ab32518; E130 clone; lot 19; RRID:AB_733068
Mouse monoclonal anti-IkBα	Cell Signaling	Cat#9246; 5A5 Clone; RRID:AB_2267145
Rat monoclonal anti- nlrp3	R&D Systems	Cat#MAB7578; Clone 768319; RRID:AB_2605972
Rabbit polyclonal anti-NLRC4	Novus Biologicals	Cat#NB100-56142; RRID:AB_838492
Rabbit polyclonal anti-AIM2	Abcam	Cat#ab93015; RRID:AB_10564699
Rabbit polyclonal anti-AIM2	Cell signaling	Cat#13095S; 12/2015; RRID:AB_2732808
Rabbit monoclonal anti-RIG-I	Cell signaling	Cat#3743; D14G6 clone; RRID:AB_226923
Mouse monoclonal anti-Caspase-1	Adipogen Life Sciences	Cat#AG-20B-0042; RRID:AB_2490248
Rabbit polyclonal anti-IL1β	Santa Cruz Biotechnology	Cat#sc-7884; H-153 clone; RRID:AB_2124476
Rabbit polyclonal anti-IL1β	Santa Cruz Biotechnology	Cat#sc-32294; lot K2117; RRID:AB_627790
Rabbit polyclonal anti-Rel A	Abcam	Cat#ab16502; RRID:AB_443394
Rabbit monoclonal anti-Rel A	Abcam	Cat#ab32536; lot GR200963-6; RRID:AB_776751
Rat monoclonal anti-MOMA-2	ABDSEROTEC	Cat#MCA519; RRID:AB_1102752
Rat monoclonal anti-F4/80	ABDSEROTEC	Cat#MCA497; RRID:AB_2098196
Rabbit polyclonal anti-ASC antibody	Santa Cruz Biotechnology	Cat#sc-22514-R; N-15; RRID:AB_2174874
Rabbit polyclonal anti-β actin	Cell Signaling	Cat#4970S; lot14; RRID:AB_2223172
Bacterial and Virus Strains		
Leishmania amazonensis LV79	Institut Pasteur Cayenne	WHO reference number MPRO/BR/72/M1841
Chemicals, Peptides, and Recombinant Proteins		
LPS	Alpha Diagnostic Intl. inc.	Cat#LPS11-1
ATP	SIGMA	Cat#A2383, CAS#34369-07-8
Hoechst 33,342	ThermoFisher Scientific	Cat#62249, CAS#*875756-97-1*
mrCSF-1	ImmunoTools	Cat#12343115, CAS#81627-83-0
Actinomycin D	SIGMA	Cat#A9415, CAS#*50-76-0*
MSSAFE	SIGMA	Cat#MSSAFE-1VL
Disuccinimidyl suberate	ThermoFisher Scientific	Cat#21555, CAS#68528-80-3
Carbobenzoxy-Leu-Leu-Leucinal (MG132)	SIGMA	Cat#M8699, CAS#1211877-36-9
Critical Commercial Assays		
SuperSignal West Pico reagent	ThermoFisher Scientific	Cat#34079
iTaq Universal SYBR® Green Supermix	Bio-Rad	Cat#172-5124
IL-1β Instant ELISA kit	eBioscience	Cat#BMS60002ISNT
TNF Instant ELISA kit TNF	eBioscience	Cat#BMS60712ISNT
IL-1α ELISA kit	eBioscience	Cat#BMS611
IL-18 ELISA kit	R&D system Europe	Cat#7625
EpiTect® ChIP qPCR Array Mouse NF-κB Signaling Pathway	QIAGEN	Cat#GM-025A
Experimental Models: Organisms/Strains		
BALB/c female mice	Janvier	BALB/cJRj
Swiss nu/nu female mice	Janvier	Rj:NMRI-nu (nu/nu)
Oligonucleotides		
Primers for RT-qPCR: see Tables S1–*S2*	SIGMA	N/A

LEAD CONTACT AND MATERIALS AVAILABILITY

Further information and requests for resources and reagents should be directed to and will be fulfilled by the lead contact Gerald F. Späth (gerald.spaeth@pasteur.fr).

This study did not generate new unique reagents.

EXPERIMENTAL MODEL AND SUBJECT DETAILS

Ethics Statement

Six-week-old female BALB/cJRj and Swiss *nu/nu* mice were purchased from Janvier (Saint Germain-sur-l'Arbresle, France) or from Shanghai Laboratory Animal Center (SLAC). All animals were housed in A3 animal facilities according to the guidelines of Institut Pasteur and the "Comité d'Ethique pour l'Expérimentation Animale" (CEEA) and protocols were approved by the "Ministère de l'Enseignement Supérieur; Direction Générale pour la Recherche et l'Innovation" under number 2013-0047 and by the Animal Care and Use Committee at Institut Pasteur of Shanghai Animal Care.

Isolation and Culture of Bone-Marrow-Derived Macrophages

Bone marrow cell suspensions were recovered from tibias and femurs of BALB/c mice in DMEM medium (GIBCO, Life technologies) and cultured in medium complemented with mouse recombinant colony stimulating factor 1 (mrCSF-1, ImmunoTools) (de La Llave et al., 2011). One million cells per ml were incubated in bacteriologic Petri dish (Corning Life Science) at 37°C in a 7.5% CO2 atmosphere for 6 days with 75 ng/mL mrCSF-1. After detachment with 25 mM EDTA, 2 million macrophages were seeded per well in 12-well plates in 2 mL culture medium containing 20 ng/mL mrCSF-1.

Inflammasome Activation in Macrophage Cultures

Inflammasome activity was analyzed after sequential treatment with 500 ng/ml LPS for 4 hours and 5 mM ATP for 2 hours. Proteasomal protein degradation was studied in presence of 10 μM carbobenzoxy-Leu-Leu-Leucinal (MG132) during 4 hours.

Parasite Isolation and BMDM Infection

mCherry transgenic, tissue-derived amastigotes of *Leishmania amazonensis* strain LV79 (WHO reference number MPRO/BR/72/M1841) were isolated from infected footpads of Swiss nude mice (Lecoeur et al., 2010). Amastigotes were added at a ratio of 4 amastigotes per macrophage, reaching 95% of infection (fluorescence microscopy analysis of Hoechst-stained samples). Metacyclic promastigotes were isolated from stationary phase amastigote-derived promastigote cultures on a discontinuous Ficoll gradient (Späth and Beverley, 2001) and added to BMDMs at a multiplicity of infection (MOI) of 8:1. Cells were cultured at 34°C for 3 to 30 days post-infection (PI). The supernatant was replaced once a week by fresh complete medium containing 20 ng/ml mrCSF-1. BMDMs were allowed to ingest heat-killed, tissue-derived amastigotes obtained after 20 min treatment at 45°C, or inert latex beads (5 μm particle size, Sigma-Aldrich) at a bead to macrophage ratio of 20:1. Phagocytic activity was determined using Texas red-labeled zymosan (ThermoFisher Scientific).

Generation of *Ex Vivo* Macrophages in BALB/c Nude Mice

Infected macrophages were generated in the footpad of 5-7 week old female BALB/c nude mice (Balb/cRj-nu, JanvierLabs) infected by *mCherry* transgenic, tissue-derived amastigotes of *Leishmania amazonensis*. Lesions were harvested for macrophage isolation 2 months post infection.

METHOD DETAILS

Isolation of *Ex Vivo* Macrophages from Mouse Lesions

Infected macrophages were isolated from footpad lesions of BALB/c nude mice obtained 2 months post-inoculation of amastigotes. Mice were euthanized by carbon dioxide inhalation, footpads were removed and placed in Digestion Buffer (DB) composed of 50 U/ml DNase I (Sigma-Aldrich), 100 U/ml collagenase II (Sigma-Aldrich), 100 U/ml collagenase IV (Sigma-Aldrich) and 1 U/ml dispase II (Roche Applied Science) in DMEM and placed on a 100 μm cell strainer. One ml of DB was perfused in the footpad at 5 different locations that were maintained at 37°C for 30 minutes. This step was repeated two times. Macrophages were recovered and washed (centrifugation at 50 *g*, 10 min, 4°C) before processing.

Western Blotting

BMDMs were lysed in RIPA buffer (R0278, Sigma-Aldrich) containing protease / phosphatase inhibitors (MS-SAFE, Sigma-Aldrich). Proteins were resolved by SDS–PAGE (4%–12% Bis-Tris NuPAGE gels, MOPS buffer), electroblotted (polyvinylidene difluoride membranes), blocked (5% fat-free milk, Tris-buffered saline, 0.25% Tween 20) and probed overnight at 4°C with anti- NLRP3 (MAB7578, R&D Systems), NLRC4 (NB100-56142, Novus Biologicals), AIM2 (ab93015, abcam), RIG-I (3743, D14G6 clone, Cell Signaling), caspase-1 p20 (AG-20B-0042, Adipogen Life Sciences), IκBα (ab32518, abcam), phospho IkBα (MA5-14857, clone

J10.3,ThermoFischer scientific), IKKβ (AM8109a, 62AT216 clone, Abgent), IKKγ (sc-8330, Santa Cruz Biotechnology) and β-actin (4970, Cell Signaling) antibodies.

To detect the ASC pyroptosome, BMDMs were lysed (50 mM Tris pH 7.5, 150 mM NaCl, 1% NP-40, MS-SAFE), and sheared 10 times through a 21-gauge needle. Lysates were cross-linked with 4 mM disuccinimidyl suberate and resolved by electrophoresis (12% SDS-PAGE). Immunoblotting was performed with anti-ASC antibody (sc-22514-R, Santa Cruz Biotechnology).

To detect released IL-1β and caspase-1, soluble proteins from supernatants were precipitated with methanol / chloroform, separated by SDS-PAGE, transferred to nitrocellulose membranes and immunoblotted with anti-IL-1β (sc-7884; Santa Cruz Biotechnology) or caspase-1 p20 (AG-20B-0042, Adipogen) antibodies.

Following incubation with peroxydase-conjugated secondary antibodies, membranes were revealed by SuperSignal West Pico reagent (ThermoFisher Scientific) (PXi machine, Syngene). Relative protein expression was calculated by densitometric analysis (ImageJ software). Ratios between integrated density values obtained for the target protein and β-actin were calculated. Fold changes were expressed using the control sample (calibrator), with control values of uninfected / unstimulated samples being set to 1.

RNA extraction and transcriptional analyses by real time quantitative PCR (qRT-PCR)

Total RNA isolation, quality control and reverse transcription were performed (de La Llave et al., 2011). qRT-PCR was carried out in 384-well PCR plates (Framestar 480/384, 4titude, Dominique Dutscher) using the iTaq Universal SYBR® Green Supermix (Bio-Rad) and 0.5 μM primers with a LightCycler® 480 system (Roche Diagnostics, Meylan, France). Primer information for every target tested by qPCR is detailed (Tables S1–S2). Crossing Point values were determined (second derivative maximum method (LightCycler® 480 Basic Software). The relative expression software tool (*REST©-MCS*) (Pfaffl et al., 2002) was used to determine relative expression as fold change (FC) values. Normalization was performed using the geometric mean of *ywhaz* and *rpl19* quantities (BMDMs) and *ppih* and *mau2* (*ex vivo* macrophages) (GeNorm and Normfinder programs). For statistical analysis of gene expression levels Cp values were first transformed into relative quantities (RQ) and normalized (de La Llave et al., 2011). Nonparametric Kruskal-Wallis tests were performed on Log transformed Normalized Relative Quantity values.

The modulation of macrophage RNA stability by *L. am* amastigotes was analyzed after Actinomycin D (AD, A9415, Sigma) treatment (5 μg/ml) in uninfected and infected samples stimulated with LPS. The modulation of RNA stability by *L. am* amastigotes was determined by comparing the FC values obtained between AD-treated versus AD-non treated cell samples.

Heatmaps of the Fold-Changes on the log2 scale (qRT-PCR) and evaluation of the differences in H3 acetylation between infected and uninfected samples were performed (R, version 3.4.3.) and home- made scripts based on native graphical functions.

Cytokine Quantitation in Culture Supernatants

Cytokines were quantified in the supernatant using mouse instant ELISA kits (for IL-1β and TNF, eBioscience) or classical mouse ELISA kits for IL-1α (eBioscience) and IL-18 (R&D system Europe).

Microscopic and Immunofluorescence Analyses

BMDMs were seeded in complete medium containing 20 ng/ml mrCSF-1 either on glass slides ($1.5x10^5$ cells in 24-well plates or $5x10^4$ cells in 96-well plates) per well. BMDMs were fixed / treated (Prina et al., 2004) and incubated in 0.1% saponin buffer containing 0.25% gelatin and anti-F4/80 (MCA497 AbD Serotec), MOMA-2 (MCA519 AbD Serotec) and RelA polyclonal antibodies (ab16502, abcam). Stainings were revealed using appropriate secondary antibodies. Nuclear staining was performed with Hoechst 33342 (ThermoFisher Scientific). Image acquisition / analysis for coverslips were performed using the upright ZEISS Axio Imager 2 (Zen Imaging Software). Image acquisition for 96-well plates was performed on the OPERA QEHS confocal microscope (Perkin Elmer Technologies, Columbus software package, PerkinElmer Technologies). Automated scoring of fluorescence signals was performed for (i) nuclear localization of p65 (RelA), (delineated by Hoechst 33342nuclear counter stain), and (ii) parasite detection using the mCherry signal. 28 fields per well were acquired (at least 800 cells analyzed per condition).

Chromatin Isolation, Chip Analysis, and qPCR

BMDMs were seeded in 100 mm tissue culture dishes. At day 3 PI, chromatin preparation, isolation, and shearing from infected macrophages were performed using a modification of a described procedure (Arrigoni et al., 2016). Cells were washed with protein-free medium (34°C), fixed (1% methanol-free formaldehyde at 34°C, 10 min), incubated 10 min in 125 mM Glycine at 4°C. Cells were scraped into Nuclei EXtraction by SONication (NEXSON) buffer (5 mM PIPES pH 8, 85 mM KCl, 0.5% Igepal CA-630) containing 2 x Halt protease inhibitor cocktail (Thermo Scientific). Samples were sonicated in 1.5 mL Eppendorf tubes using the Bioruptor device (Diagenode) at ''low power'' with two cycles (30'' on 30'' off). Macrophage nuclei isolation was microscopically evaluated before collection of the nuclei by centrifugation (5 min, 4°C, 2000*g)* and resuspension in shearing buffer (10 mM Tris-HCl pH 8, 0.1% SDS, 1 mM EDTA, 2 x Halt protease inhibitor cocktail). Chromatin was sheared into 100-500 bp fragments (three 5 min ultra-sound pulses, 4°C, sonicator set at ''high power''). Chromatin immunoprecipitations were performed with the EpiTect® ChIP OneDay Kit (QIAGEN) using control IgGs and antibodies against acetylated histone H3 (H3K9/14ac) and tri-methylated H3K4 and H3K9 (diagenode). The EpiTect® ChIP qPCR Array Mouse NF-κB Signaling Pathway was applied on (i) 1/100 of the input material before immunoprecipitation (positive control), (ii) negative control IgGs from normal non-immune serum (background assessment), and iii) H3ac fractions (epigenetic status for genes of the NF-κB pathway). qPCR data were obtained on a LightCycler® 480 system (Roche

Diagnostics, Meylan, France) using the 384-well template (GM-025G, QIAGEN), and were expressed as percent of input for every target gene in uninfected and infected BMDMs. The distance between H3 acetylation levels in NF-κB related promoters and the corresponding bisector was analyzed for *L. am*-infected versus non-infected BMDMs, in presence or not of LPS.

QUANTIFICATION AND STATISTICAL ANALYSIS

Statistical Analysis

Analysis of gene expression levels determined by RT-qPCR were performed with SigmaPlot for Windows Version 11.0, Build 11.2.0.5 and was expressed as mean values ± SEM. Statistical details of experiments are provided in legends of every corresponding figure. Statistical analyses were performed by the nonparametric Wilcoxon rank-sum test H (GraphPad Prism 7.03 software).

DATA AND CODE AVAILABILITY

This study did not generate any unique datasets or codes